SEARCHING FOR NEUTRAL KAONS IN THE SHIP TEST BEAM DATA

A THESIS SUBMITTED TO
THE GRADUATE SCHOOL OF NATURAL AND APPLIED SCIENCES
OF
MIDDLE EAST TECHNICAL UNIVERSITY

BY

ONUR DURHAN

IN PARTIAL FULFILLMENT OF THE REQUIREMENTS
FOR
THE DEGREE OF MASTER OF SCIENCE
IN
PHYSICS

SEPTEMBER 2020

Approval of the thesis:

SEARCHING FOR NEUTRAL KAONS IN THE SHIP TEST BEAM DATA

submitted by **ONUR DURHAN** in partial fulfillment of the requirements for the degree of **Master of Science in Physics Department, Middle East Technical University** by,

Prof. Dr. Halil Kalıpçılar
Dean, Graduate School of **Natural and Applied Sciences** _____

Prof. Dr. Altuğ Özpineci
Head of Department, **Physics** _____

Prof. Dr. Ali Murat Güler
Supervisor, **Physics, METU** _____

Examining Committee Members:

Prof. Dr. Orhan Çakır
Physics, Ankara University _____

Prof. Dr. Ali Murat Güler
Physics, METU _____

Prof. Dr. Altuğ Özpineci
Physics, METU _____

Prof. Dr. İsmail Turan
Physics, METU _____

Assoc. Prof. Dr. Deniz Yılmaz
Physics Engineering, Ankara University _____

Date:

I hereby declare that all information in this document has been obtained and presented in accordance with academic rules and ethical conduct. I also declare that, as required by these rules and conduct, I have fully cited and referenced all material and results that are not original to this work.

Name, Surname: Onur Durhan

Signature :

ABSTRACT

SEARCHING FOR NEUTRAL KAONS IN THE SHIP TEST BEAM DATA

Durhan, Onur
M.S., Department of Physics
Supervisor: Prof. Dr. Ali Murat Güler

September 2020, 53 pages

The SHiP experiment at the CERN-SPS is proposed to explore the new physics beyond the Standart Model. While delivering intense proton beam from SPS, SHiP combines several detector technologies with dedicated background rejecting systems to discover new particles and interactions. In order to estimate the background yield from muons, a test beam exposure was done, in July, 2018 at CERN. In addition to muons, V0 decays constitute the major background for the SHiP experiment. Among these, neutral kaon decays, in particular, have the potential to mimic the signal as they have very similar decay topology and final state particles with decays of so-called hidden particles. This thesis work is on the study of $K_S \to \pi^+\pi^-$ decays using both Monte Carlo simulations and the data collected at the muon flux test beam for SHiP .

Keywords: K_S^0, Muon Flux Measurement, SHiP, Test Beam

ÖZ

SHİP TEST IŞINIMINDA YÜKSÜZ KAON ARAŞTIRMASI

Durhan, Onur
Yüksek Lisans, Fizik Bölümü
Tez Yöneticisi: Prof. Dr. Ali Murat Güler

Eylül 2020 , 53 sayfa

SHiP Standart Model ötesi yeni fizik kuramlarını test etmek için CERN-SPS'te yeni bir deney kurulmasını teklif etmiştir. SHiP deneyi bu araştırmaların gerçekleşmesi için, SPS hızlandırıcılarının yoğun protonlarından beslenirken, yeni dedektör teknolojilerini güçlü arkaplan önleyici sistemlerle bütünleştirmeyi hedeflemektedir. Muonların oluşturacağı arkaplanı hesaplamak için CERN'de, Temmuz 2018'de test ışınım ölçümleri gerçekleşmiştir. Ayrıca, SHiP deneyi için V0 bozunumları başlıca arkaplan kaynakları arasındadır. SHiP deneyinde, özellikle yüksüz kaon bozunumları yeni fiziğe ait sinyali taklit etme potansiyeline sahiptir. Bu tez, $K_S \to \pi^+\pi^-$ bozunumlarının, Monte Carlo simülasyonları ve SHiP muon test verisi kullanılarak araştırılması hakkındadır.

Anahtar Kelimeler: K_S^0, Muon Akısı Ölçümü, SHiP, Demet Testi

To my family

ACKNOWLEDGMENTS

I gratefully acknowledge TAEK for supporting our project "Testing Beyond the Standart Model Theories at CERN and Development of Emulsion Based Detectors" (project no: 2018TAEK(CERN)-A5.H6.F2-17). I would like to thank all my colleagues at METU whom I shared my excitement of our first test beam experience at CERN, notably, Atakan Tuğberk Akmete who helped me through becoming a user of the FairShip software and lxplus of CERN. As well, I would like to thank Oliver Lantwin for his kind helps through software. Furthermore, I would like to express my special thanks of gratitude to Thomas Ruf and Eric van Hervijnen. I would like to also thank all my friends and my family. Last but not least, I would like to express my deep and sincere gratitude to Prof. Dr. Ali Murat Güler, who supervised this thesis, encouraging me with his wisdom since from my undergraduate years.

TABLE OF CONTENTS

ABSTRACT v

ÖZ vi

ACKNOWLEDGMENTS viii

TABLE OF CONTENTS ix

LIST OF TABLES xii

LIST OF FIGURES xiii

LIST OF ABBREVIATIONS xvi

CHAPTERS

1 INTRODUCTION 1

2 STANDART MODEL AND BEYOND 3

2.1 The Standart Model 3

2.2 Need for New Physics 5

2.3 Portals to the Hidden Sector 7

2.3.1 Vector Portal 7

2.3.2 Scalar Portal 8

2.3.3 Neutrino Portal 9

3 THE SHIP EXPERIMENT 11

3.1 The SHiP Facility 11

3.2 Conceptual Design 12
3.2.1 The SHiP Spill 13
3.2.2 The SHiP Target 14
3.2.3 Muon Shield 15
3.2.4 Scattering and Neutrino Detector (SND) 15
3.2.5 Decay Volume 17
3.2.6 Spectrometer and Calorimetry 18
3.3 The SHiP Software: FairShip 18
4 MEASUREMENT OF MUON FLUX FOR SHIP 19
4.1 Experimental Setup 19
4.1.1 The Target 21
4.1.2 The Hadron Absorber 21
4.1.3 Drift tubes 21
4.1.3.1 $r - t$ Calibration 24
4.1.4 Resistive Plate Chambers (RPC) 25
4.2 Data 26
4.3 The Momentum Measurement 27
4.4 Track Reconstruction 30
5 SEARCH FOR $K_S^0 \to \pi^+\pi^-$ IN THE SHIP TEST BEAM DATA 33
5.1 MC Simulation with Muon Deep Inelastic Scattering 34
5.1.1 Number of Expected DIS Events 35
5.1.2 K_S^0 Kinematics 38
5.1.2.1 Armenteros-Podolanski Distribution 38

5.1.3 Invariant K^0_S Mass 39
5.1.3.1 Aside : Muon DIS Full Simulation 41
5.1.3.2 Coplanarity 42
5.1.4 Reconstruction of Pion Tracks 43
5.1.5 Identification of Pions 44
5.2 Data 46
5.2.1 Track Selection 46
5.2.2 Invariant Mass 47
6 CONCLUSION 49
REFERENCES 51

LIST OF TABLES

TABLES

Table 4.1 Three different magnetic field configurations. 26

Table 4.2 Data taken with three different fields. 26

Table 5.1 Table showing the signal and background channels. DP = Dark Photon, HNL = Heavy Neutral Lepton, PNGB= Pseudo-Nambu Goldston Boson, HP= Higgs Portal. 34

Table 5.2 The number of hits per each station due to $\sim$ 448k true pion tracks originated from K^0_S. 44

Table 5.3 Table showing the origins of tracks per 10^6 POT in MC. 47

LIST OF FIGURES

FIGURES

Figure 2.1 The Standard Model of particle physics. 4

Figure 2.2 Frontiers of experimental high energy physics. Intensity frontier: suitible to test weak interactions. Energy frontier: suitible to search for high masses. 6

Figure 2.3 Fermions of Standard Model with three new active neutrinos. . . 9

Figure 3.1 The location of the SHiP facility.[1] 11

Figure 3.2 The location of the SHiP facility.[1] 12

Figure 3.3 The layout of the SHiP experimental design as it is in the comprehensive design study (CDS) [2]. A diagram of the HNL decay inside the vessel is also shown. 13

Figure 3.4 A quasi-trapezoidal spill with good uniformity. 13

Figure 3.5 Energy deposition peaks during a spill. Figure adapted from [1]. 14

Figure 3.6 Target layout. Figure adapted from [1]. 15

Figure 3.7 Left: the $x-z$ view of a possible active muon shield. The trajectory of two 350 GeV muons with a range of initial angles is shown. The blue and green regions show field and return field respectively. Right: same with 30 GeV muons. Adapted from [1]. 16

Figure 3.8 Top view of the Muon Shield. 16

Figure 3.9 Side view of the Muon Shield. 16

Figure 3.10 SND configuration. 17

Figure 3.11 The vacuum vessel. 17

Figure 4.1 The spectrometer layout and the coordinate system as implemented in the FairShip. 20

Figure 4.2 The stereo structure of modules of T1 and T2. 20

Figure 4.3 Energy loss of particles in several media.[3] 22

Figure 4.4 Illustration of avelanche formation.[3] 23

Figure 4.5 A TDC distribution of group of 12 channels of T4 24

Figure 4.6 RT relations 25

Figure 4.7 Illustration of signal formation in RPC. 25

Figure 4.8 Illustration of trajectory of a charged particle in a magnet. Figure adapted from the reference. [3] 27

Figure 4.9 Illustration of maximum deflection angle 29

Figure 4.10 The B_y component as a function of y and z at $x = 1.4m$ with respect to the center of Goliath. 29

Figure 4.11 B_y as a function of z at x=1.4 m, y=0. in the Goliath reference frame. 30

Figure 4.12 The momentum resolution as function of momentum for two values of spatial resolution. 31

Figure 5.1 The diagram showing the muon deep inelastic scattering. [4] . . 35

Figure 5.2 The momentum distribution of muons used as input in the DIS simulation. 36

Figure 5.3 The momentum distribution of K^0_S from PYTHIA6. 36

Figure 5.4 The flight length distribution of K^0_S. 37

Figure 5.5 A $K^0_S \to \pi^+\pi^-$ event in the event display. 37

Figure 5.6 The Armenteros-Podolanski distribution of MC $K^0_S \to \pi^+\pi^-$ events. 38

Figure 5.7 Left: Invariant mass vs. vertex position. Right: Invariant mass. Incorrect vertices can be seen. 39

Figure 5.8 Reco vs. True vertex positions. 40

Figure 5.9 The minimum distance between two tracks from K^0_S decays. . . 40

Figure 5.10 Invariant K^0_S mass for MC. Left: nominal field, right: intermediate field. The number of reconstructed events is larger for the intermediate field. 41

Figure 5.11 Invariant mass distribution of two pion events. The contribution from K^0_S is not visible. 42

Figure 5.12 Coplanarity angle distribution. Reconstructed pion direction and true K^0_S are used. 43

Figure 5.13 Reconstructed versus True momentum of pions from K^0_S decays. 44

Figure 5.14 The true momentum distribution of pions before entering the magnet. i.e. the momentum at T2. 45

Figure 5.15 Momentum distributions of pion candidates in POT MC and data. The momentum distribution of true pion tracks is also shown. . . . 46

Figure 5.16 Invariant mass-data. 48

LIST OF ABBREVIATIONS

ABBREVIATIONS

SM	Standard Model
SHiP	Search for Hidden Particles
BSM	Beyond the Standard Model
LHC	Large Hadron Collider
SPS	Super Proton Synchrotron
BDF	Beam Dump Facility
SND	Scattering and Neutrino Detector
DIS	Deep Inelastic Scattering
HS	Hidden Sector
HNL	Heavy Neutral Leptons
DP	Dark Photon
HP	Higgs Portal

CHAPTER 1

INTRODUCTION

The standard model (SM) is a beautiful theoretical model that describes the elementary particles and their interactions. Even though it is quite successful at explaining how the universe works and has countless achievements including the discovery of the Higgs Boson in 2012 at CERN, there are still questions yet to be answered in nowadays physics. The Dark Matter (DM), the neutrino masses-oscillations, and the baryon asymmetry in the universe rank as top among these questions. There are theories the so- called Beyond the Standard Model (BSM) theories suggesting that these mysteries can be illuminated by extending the SM with new particles. Two approaches are adopted by the current sense of today's experimental high energy physics: the energy frontier approach and the intensity frontier approach. New physics is being tested by conducting experiments at the so-called energy frontier -operation at higher energies to discover higher mass particles or at the so-called intensity frontier at which a vast amount of interactions are produced at lower energies to observe weakly interacting lower mass particles. Either at the energy frontier or the intensity frontier, it is quite obvious that new techniques and sensitive detectors are essentials to sail to deep oceans of particle physics.

The SHiP experiment is a novel experiment dedicated to search for hidden particles such as dark photon (DP), heavy neutral leptons (HNL) through direct detection of their decay products, or light dark matter (LDM) through the scattering of atoms at the intensity frontier by isolating these rare events.

It naturally arises that one of the major challenges for the SHiP experiment is to reduce the background to a zero so that aforementioned rare events can be observed. Monte Carlo (MC) studies suggest that among many sources muons constitute the

primary background. Therefore, in 2018, a test beam exposure in which we have participated as the METU SHiP team has been done to measure the muon flux emanating from the SHiP target by impinging on 400 GeV protons. The 400 GeV proton beam has been delivered from the SPS accelarator to a replica of the SHiP target installed at the H4 beamline area at CERN. The reconstruction and analysis of the test beam data have been done in the following years. In addition to muons, the so-called V0 decays constitute another background source for SHiP new physics searcheas as their decay topologies and the final states are quite similar with the SHiP's signal. Moreover, these V0 decays could be induced by muons via deep inelastic scattering process. The tracking detectors of the test beam setup were suitable to get the momentum spectra of long-lived charged hadrons such as pions.

An interesting task would be then is to study the so-called V0 decays, that have the potential to mimic the signal, in particular K_S^0 decaying into two oppositely charged pions. With this motivation, in this thesis, K_S^0 events have been studied using both Monte Carlo simulations and the muon flux test beam data. This thesis is organized as follows:

- In Chapter 2 a general overview of the current status in the particle physics, the Standart Model and beyond will be provided.
- In Chapter 3 a general overview of the SHiP facility and the SHiP concept will be described.
- In Chapter 4 motivation and experimental layout of the muon flux measurement, the status of the collected data and the track reconstruction will be described.
- In Chapter 5, the production, reconstruction, and analysis of the K_S^0 events along with the muon deep inelastic scattering, Monte Carlo simulation will be reported.The expected number of the muon DIS events will be estimated and the simulation results will be compared with the data.
- In Chapter 6, finally, the summary and conclusion of this work will be given.

CHAPTER 2

STANDART MODEL AND BEYOND

2.1 The Standart Model

The Standart Model (SM) of particle physics comprises our knowledge and best understanding of the nature. It describes the elementary particles and their interactions. According to the SM, elementary particles are categorised as fermions (spin-$1/2$ particles) that constitute the matter in the universe, and bosons (spin integer particles) that mediate forces between them. Three types of fundamental forces are introduced by the SM: strong, electromagnetic and weak. The gravitational force is not included by the SM.

Fermions of the SM are divided into two subsets: leptons and quarks. Each lepton and quark is assoicated with its anti-particle i.e. the same particle with opposite intrinsic quantum numbers.

The lepton family constists of three charged leptons each of which associated with a neutral one-neutrinos. Then, six members of the lepton family are introduced as

- the electron (e^-) and the electron neutrino (ν_e)
- the muon (μ^-) and the muon neutrino (ν_μ)
- the tau (τ^-) and the tau neutrino (ν_τ)

In the SM, each lepton comes with a lepton number (l) i.e. for leptons $l = 1$ for anti-leptons $l = -1$ and for any other particle $l = 0$. The lepton number is a conserved quantity in every elementary processes. For example in the decay of the neutron an

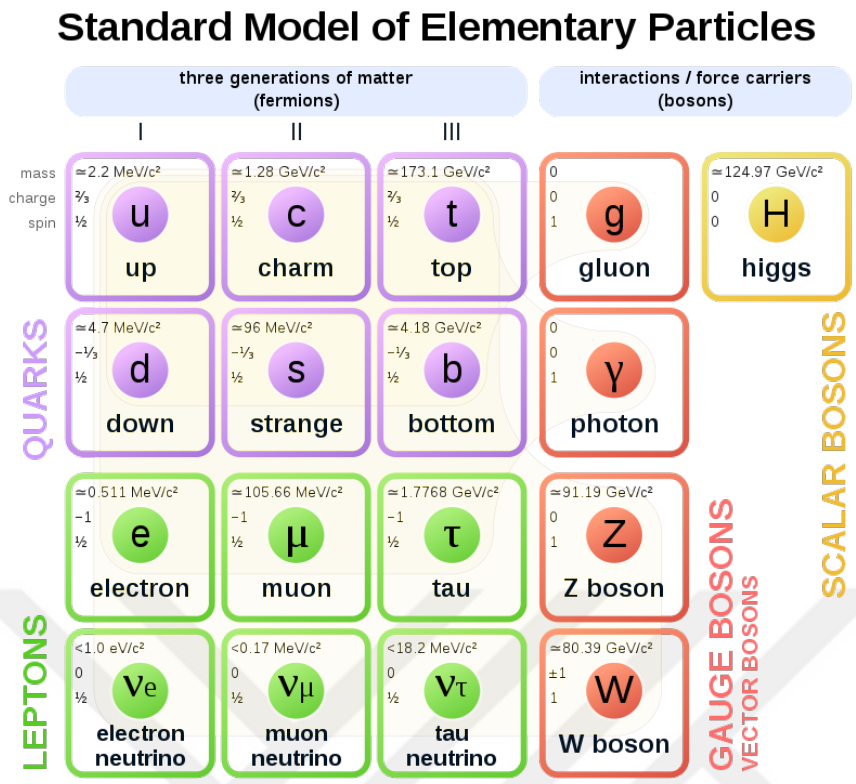

Figure 2.1: The Standard Model of particle physics.

electron anti-neutrino, not electron neutrino, is emitted along with the proton and the electron.

As far as quarks are concerned, six types of quarks are introduced by the SM: up (u), down(d), charm (c), strange (s), top(t), and bottom(b). As well as making the nuclie of atoms, protons and neutrons that is what planets and starts are made of, quarks have never been observed as a single particle. They are always found in bound states: Baryons or Mesons. Baryons are basically the combination of three quarks, for examle, the proton is made up from two up and one down quarks (uud). Every baryon comes with a baryon number (B) which is another conserved quantity in known interactions. An exquisite example of this is the decay of the proton: the proton cannot decay as there is no baryon lighter than the proton.

Mesons, on the other hand consist of two quarks. Kaons ($d\bar{s}$) and Pions ($u\bar{d}$) that we will also refer a lot in this thesis, exemplify mesons. In addition to baryons and mesons, more than three bound states of quarks, usually referred to tetraquarks and

pentaquarks, are observed [5].

So far, the matter constiuents, quarks and leptons are introduced. The SM describes their interactions with strong, electromagnetic and weak forces. γ, Z, $W^{\pm}$ and g are bosons that are messengers of these forces. The photon (γ) is responsible for the mediation of the electromagnetic force. Z and $W^{\pm}$ bosons are mediators of the weak interaction, and the strong force is mediated by the gluon (g).

Electromagnetic force is formulated under Quantum Electro Dynamics (QED) that deals with the interaction of fermions via photon exchange. Furthermore, the existence of anti-particle is predicted by QED.

The strong force is formulated by the Quantum Chromodynamics (QCD). Unlike the photon, the gluon can interact with another gluon with respect to its so-colled color charge, that is, why the theory is entitled as "Chromodynamics". The consequence of the self interaction is the quark confinement that we mentioned earlier. It leads to asymptotic freedom of quarks, inhibiting the existence of a free quark.

Unlike the gluon and the photon mediators of the weak force, $W^{\pm}$ and Z have non-zero masses. Furthermore, they can mediate charged interactions as well as neutral interactions. Nuclear beta decay, muon decay and any process that involves neutrinos are examples of weak interactions. The electromagnetic and the weak force are unified into one fundamental interaction as the "Electroweak" force after proposed by the Glashow-Weinberg-Salam unification theory.

Finally, the last pice of the SM, the Higgs Boson, is a scaler (spin-0) particle responsible for particles to obtain masses and making the SM "gauge invariant" theory i.e. it remains unchanged under symmetry transformations.

2.2 Need for New Physics

The last piece of the SM's particle collection "the Higgs" has been discovered by at the Large Hadron Collider (LHC) accelerators operating at 7-8 TeV at CERN. Despite the success of the SM through history, SM is an incomplete theory. No explanation is given by the SM for the following existing problems:

- Neutrino masses: Neutrino oscillations have been observed [6] which indicates that neutrinos have masses different than zero.

- Baryon asymmetry of the universe: There is matter-antimatter imbalance in the universe. What makes matter dominates over antimatter ? [7]

- Dark matter: Astrophysical observations indicates a large amount of mass is missing in the univerve [8]

These are some problems known as Beyond the Standard Model (BSM) problems. Particles and interactions which are yet to be explored might solve these problems. Various experiments are striving to observe heavy particles at the energy frontier such as the ones at LHC. The challenge, on the other hand, might not be due to their heavy mass but due to their very weak interaction strength with the ordinary matter. In this scenario, these particles could be probed with the experiments at the intensity frontier. It is also possible that these new particles can have larger masses and do not directly interact with ordinary particles. These "hidden particles" might be accessible at the intensity frontier via lighter particles- "portals" which interact very weakly with ordinary matter. The diagram in Figure 2.2 shows realms of two frontiers.

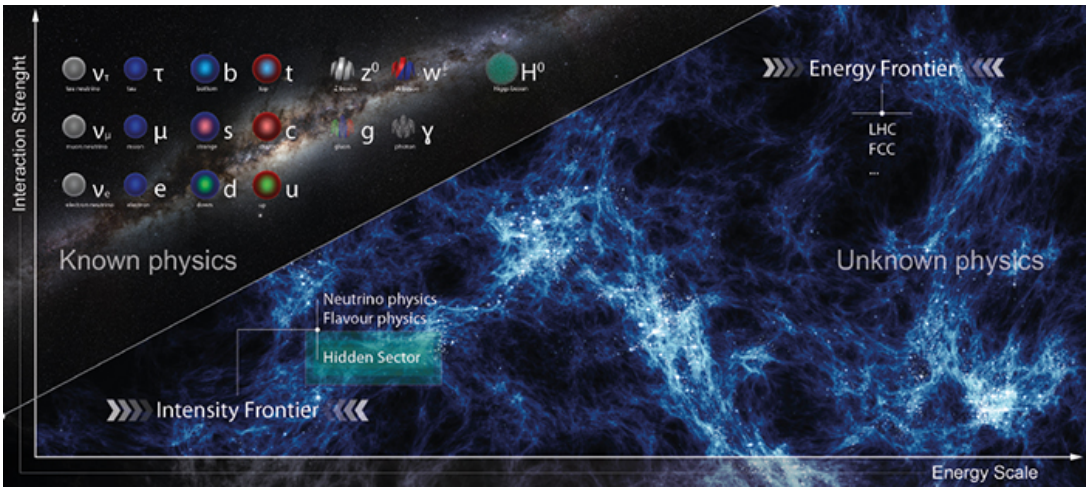

Figure 2.2: Frontiers of experimental high energy physics. Intensity frontier: suitible to test weak interactions. Energy frontier: suitible to search for high masses.

2.3 Portals to the Hidden Sector

To find solutions to BSM problems, the SM could be extended. This would result in new terms in the Lagrangian. One can write the resulting Lagrangian in a way that involves SM terms, terms that mix the SM with the Hidden Sector i.e. the portal term, and terms that belong to the Hidden Sector. Here are three portals that could access to the Hidden Sector: [9]

- Vector Portal: Abelian fields, A'_μ with field strength $F'_{\mu\nu}$
- Scalar Portal: Scalars S coupling to the square of Higgs doublet $H^\dagger H$
- The Neutrino Portal: Operators $(\bar{L}_\alpha \cdot \tilde{\Phi})$ coupling to the new N_I fermions N_I

2.3.1 Vector Portal

It is possible that the SM is accompanied by additional $U(1)$ symmetry transforming its gauge structure from $SU(3) \times SU(2) \times U(1)$ into $SU(3) \times SU(2) \times [U(1)]^2$.

In that case, one can combine two QED-type Lagrangians one of which belongs to the Hidden Sector with the vector field A'_μ analogous to the photon in QED commonly referred to the "dark photon" with a cross term $\frac{\epsilon}{2} F^{\mu\nu} F'_{\mu\nu}$ that mixes the SM with the HS.

$$\mathcal{L} = \mathcal{L}_{\psi,A} + \mathcal{L}_{\chi,A'} - \frac{\epsilon}{2} F^{\mu\nu} F'_{\mu\nu} + \frac{1}{2} m^2_{A'} \left(A'_\mu\right)^2 \tag{2.1}$$

where ϵ is the dimensionless coupling constant between SM and HS, $\mathcal{L}_{\psi,A}$ and $\mathcal{L}_{\chi,A'}$ are QED-type Lagrangians defined as

$$\mathcal{L}_{\psi,A} = -\frac{1}{4} F^2_{\mu\nu} + \bar{\psi} \left[\gamma^\mu \left(i\partial_\mu - eA_\mu\right) - m_\psi\right] \psi \tag{2.2}$$

$$\mathcal{L}_{\chi,A'} = -\frac{1}{4} \left(F'_{\mu\nu}\right)^2 + \bar{\chi} \left[\gamma^\mu \left(i\partial_\mu - eA'_\mu\right) - m_\chi\right] \chi \tag{2.3}$$

Here $F_{\mu\nu}$ and $F'_{\mu\nu}$ represent field strength tensors of the QED and the dark analog of the QED, respectively. While ψ fields are electron fields in the QED, χ fields are charged under the $U(1)'$. Writing Maxwell's equation, $\partial^\mu F_{\mu\nu} = eJ_\nu^{EM}$ the cross term can be rewritten as

$$-\frac{\epsilon}{2}F^{\mu\nu}F'_{\mu\nu} = A'_\mu \times (e\epsilon)J^\mu_{EM} \tag{2.4}$$

The equation 2.4 shows that the new vector field couples to the EM current with a strength reduced by a factor of ϵ.

The sensitivity of the SHiP experiment to the Dark Photon for several production mechanisms e.g. QCD, meson decay, Bremsstrahlung and Cascade are under study by the SHiP collaboration. [10]

2.3.2 Scalar Portal

The discovery of Higgs Boson at CERN-LHC showed that elementary scalar bosons do exist in nature and therefore provided motivation to search for other elementary scalars. There are many extensions of the SM that predict these additional fields through the Higgs sector. The Lagrangian term representing the portal through Higgs field in the most general form reads:

$$\mathcal{L}_{ScalarPortal} = (\alpha_1 S + \alpha S^2)(H^\dagger H) \tag{2.5}$$

Here α_1 and α_2 are the couplings to the Higgs doublet.

If dark matter exists it should interact with ordinary matter very weakly. Thus, the Higgs Portal could play a central role in the dark sector. One might even speculate that such scalars are themselves constitute the dark matter.

2.3.3 Neutrino Portal

The neutrino portal is defined as the coupling of one or several new fermion states $N_I(I = 1, 2, .., \mathcal{N})$ that are invisible to the SM gauge interactions to the operator $\bar{L}_\alpha \cdot \tilde{\Phi}$. The Lagrangian term representing the neutrino portal reads:

$$\mathcal{L}_{NeutrinoPortal} = F_{\alpha I}(\bar{L}_\alpha \cdot \tilde{\Phi})N_I + h.c. \tag{2.6}$$

where $F_{\alpha I}$ denotes a dimensionless Yukawa coupling L_α is the left- handed lepton doublet with the flavor index $\alpha = e, \mu, \tau$. As N_I do not feel SM gauge interactions they are commonly referred to sterile neutrinos. The extended part of the modifed SM is presented in Figure 2.3

A neutrino Minimal Standart Model (ν MSM) offers three active Ns corresponding to each neutrino generation in the SM. In this model one of the mass eigenstates has mass $\mathcal{O}(10keV)$, and other two have masses $\mathcal{O}(1GeV)$. While nominating the lighter one as a warm dark matter candidate other two could solve the baryon asymmetry via leptogenesis.

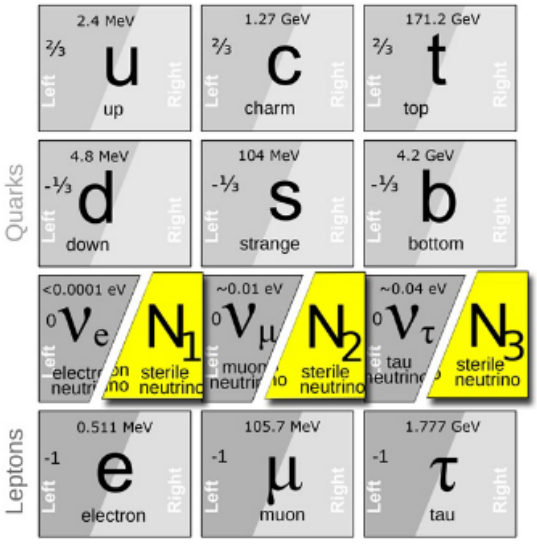

Figure 2.3: Fermions of Standard Model with three new active neutrinos.

CHAPTER 3

THE SHIP EXPERIMENT

3.1 The SHiP Facility

The SHiP collaboration proposes a new beam dump facility (BDF) to be constructed at TT20 transfer line feeding on 400 GeV protons of SPS accelerators near the Perevessin site at CERN. The sensitivity of the SHiP experiments demands a total of 2×10^{20} POT. It is expected that SPS will deliver 4×10^{19} POT per year.[1]. The geographic location of the new facility is depicted in Figure 3.1 and Figure 3.2.

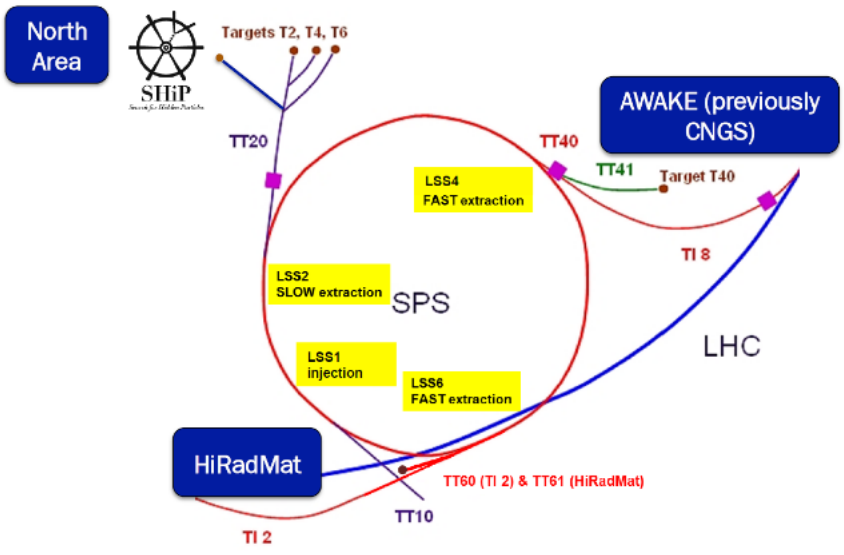

Figure 3.1: The location of the SHiP facility.[1]

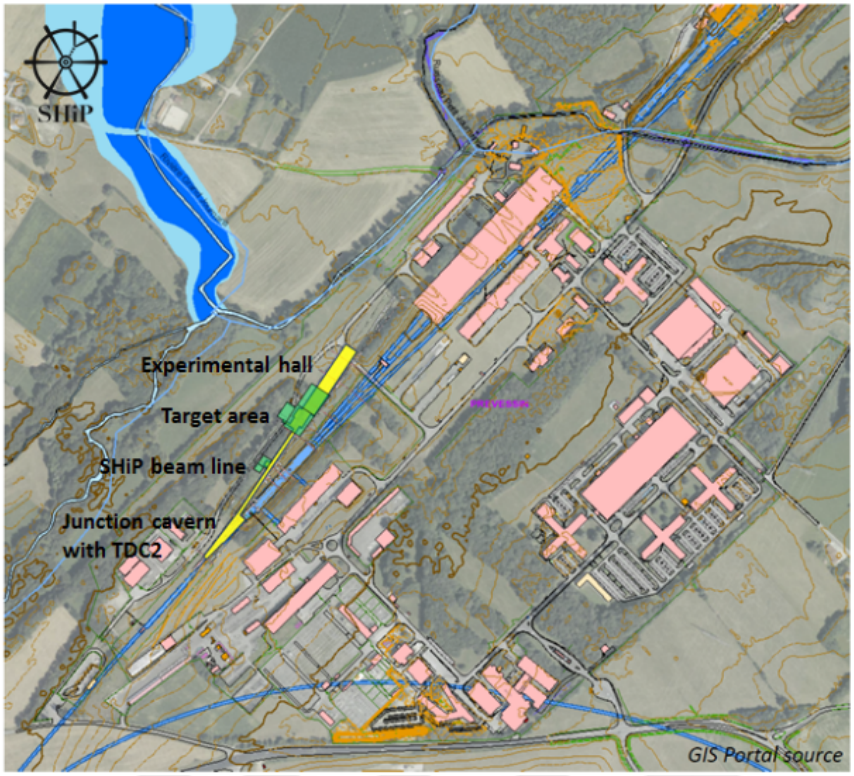

Figure 3.2: The location of the SHiP facility.[1]

3.2 Conceptual Design

The SHiP experiment aims at exploring hidden particles and SM extensions involving weakly interacting long-lived particles through the detection of their decays to SM particles. In order to achieve this goal, a new Beam Dump Facility (BDF) at CERN in the Perevessin site was proposed in 2015 [1]. The facility is dedicated to reject backgrounds by stopping hadrons, electrons, photons, sweeping out muons and curtaining the detectors from stray particles coming from outside.

The proton beam of 400 GeV energy with high intensity is planned to be delivered to the SHiP target which is an alloy of Tungsten and Molybdenum. It is expected to deliver $\sim 2 \times 10^{20}$ protons on target after operating five years. The SHiP experimental setup, from upstream to downstream, is planned to be installed as follows: The target is followed by a magnetized hadron absorber whose task is to stop hadrons emanating from the target. An active muon shield comes after the absorber to sweep out muons. The muon shield is one of the most salient components for SHiP. It's combination

of several magnets that generates strong magnetic fields in order to deflect and reject muons before entering the SHiP detector. At the downstream of the muon shield the scattering and neutrino detector (SND) is located. A vacuum vessel, hosts and isolates the hidden particle decay, is after the SND. Spectrometer and calorimeters are located at the end, measuring the momentum and making the identification of product of hidden particle decays occurring inside the vacuum vessel. The layout of the SHiP experimental design is shown in Figure 3.3.

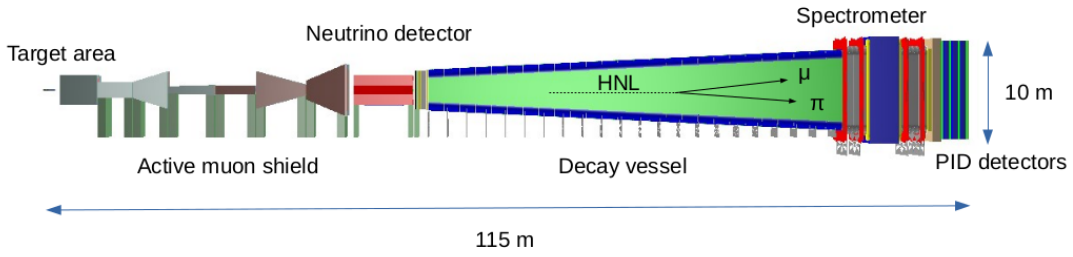

Figure 3.3: The layout of the SHiP experimental design as it is in the comprehensive design study (CDS) [2]. A diagram of the HNL decay inside the vessel is also shown.

3.2.1 The SHiP Spill

The SHiP spill from SPS is planned to contain 4×10^{13} 400 GeV protons and will be delivered to the target with the slow extraction. It's essential for SHiP to have a spill as uniform as possible. It's therefore needed to create a large momentum spread and de-bunching in the beam. The estimated beam loss during the extraction is about $1 - 5\%$.

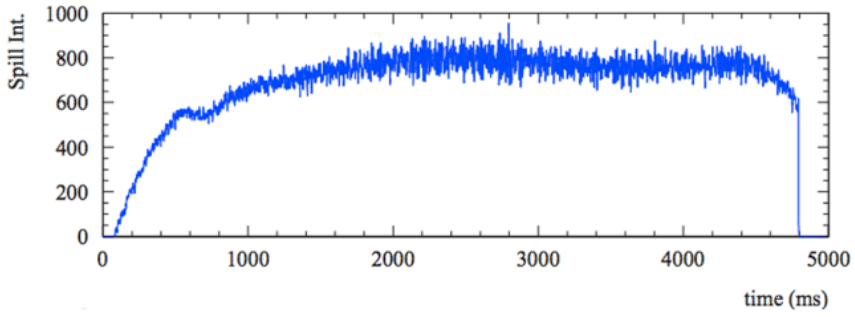

Figure 3.4: A quasi-trapezoidal spill with good uniformity.

In Figure 3.4 a not-perfectly trapezoidal spill is shown. An initial spike in the proton rate is observed in this spill. Such a spike might have an impact on the energy deposition in the target and this instantaneous increase in the beam could increase the probability of unexpected backgrounds. It's therefore needed to have a spill as perfect trapezoidal as possible. SHiP puts effort into these engineering subjects providing a facility for general purpose.

3.2.2 The SHiP Target

Hidden particles are expected to be produced via decays of the heavy hadrons. The SHiP target is designed in a way that maximizes the production of heavy mesons and minimizes the production of muons and neutrinos. The former is the source and the letter yields the background. It is therefore needed to use materials with the shortest possible nuclear interaction length and to have a volume in which the proton shower is contained. The average beam power deposited on the SHiP target during a spill is estimated to be up to 350 keV [1]. The energy deposition in the target is shown Figure 3.5. A water cooling system, as the consequence of this, is placed between each block of the target. Titanium-Zirconium doped with molybdenum blocks followed by pure tungsten blocks meet the desired material requirement. The layout of the target is presented in Figure 3.6.

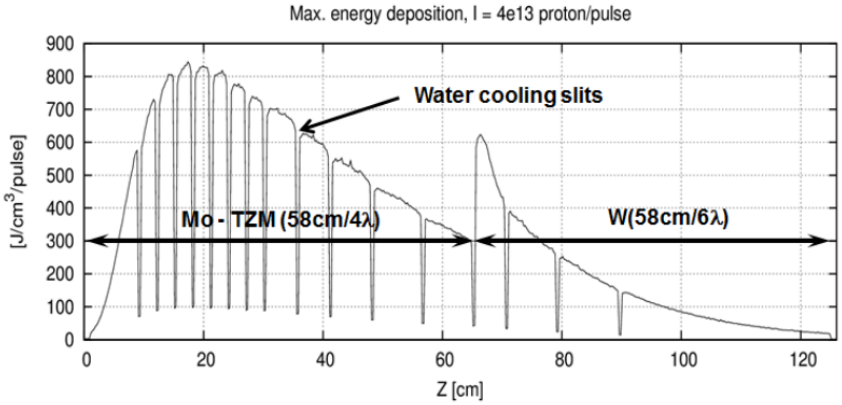

Figure 3.5: Energy deposition peaks during a spill. Figure adapted from [1].

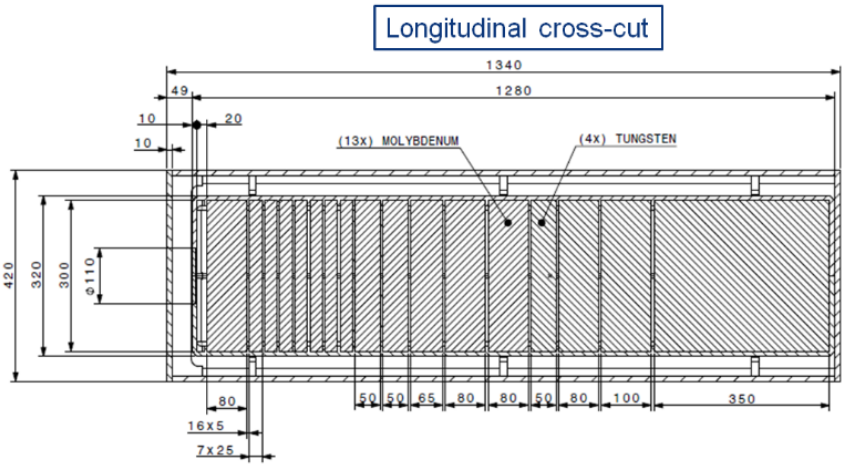

Figure 3.6: Target layout. Figure adapted from [1].

3.2.3 Muon Shield

It is expected to yield $\sim 5 \times 10^9$ muons per spill [1] for the SHiP experiment. The muon flux measurement, done with POT corresponding $\%1$ of a SHiP spill, revealed that 710 ± 15 POT/muon event is reconstructed [11]. A dedicated shielding is therefore needed. In order to preserve the acceptance, the shield should be as short along the beamline as possible. Solutions to have an optimized muon shield are still under study by the SHiP collaboration. Figure 3.7 shows trajectories of muons in a possible shield. Figure 3.8 and 3.9 is top and side view of the muon shield as implemented in the SHiP software.

3.2.4 Scattering and Neutrino Detector (SND)

The techniques used in the Scattering and Neutrino Detector (SND) is very similar to the one in OPERA [12]. The SND is a combination of several subdetectors: Emulsion target, target trackers, and muon system. The layout of the SND configuration is shown Figure 3.10. The SND emulsion target made of emulsion cloud chambers (ECC) is suitable for τ physics due to its high spatial resolution. It's also suitable for Light Dark Matter (LDM) searches. The target tracker system, on the other hand, consists of scintillating fiber detectors (SciFi) whose spatial resolution is up to 50 μm. Its purpose is to match tracks coming from the target. Finally, the muon system

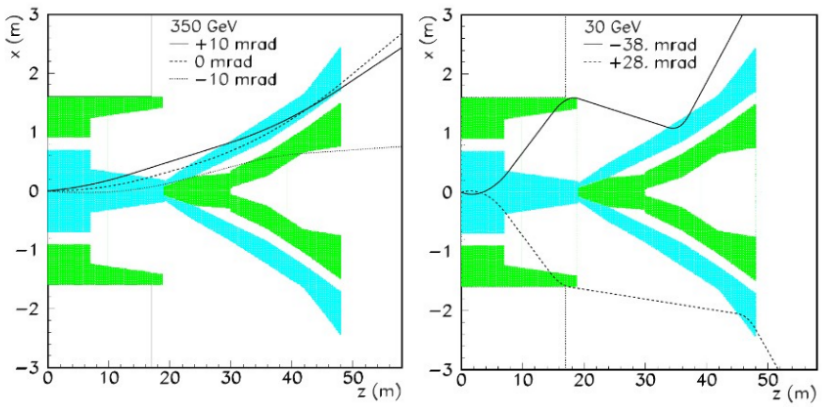

Figure 3.7: Left: the $x - z$ view of a possible active muon shield. The trajectory of two 350 GeV muons with a range of initial angles is shown. The blue and green regions show field and return field respectively. Right: same with 30 GeV muons. Adapted from [1].

Figure 3.8: Top view of the Muon Shield.

Figure 3.9: Side view of the Muon Shield.

is placed at the end to tag muons and measure their charge and momentum. This configuration also acts as a veto tagger, vetoing backgrounds without needing extra detector at the upstream of the decay volume. Aside from this, the SND is also proposed as another independent experiment [13]. It's planned to be installed near ATLAS at CERN. The neutrino beam is going to be provided from ATLAS's proton collisions.

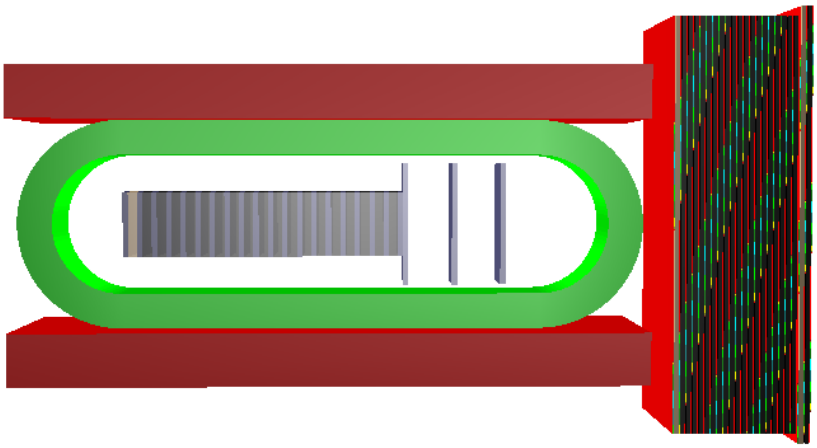

Figure 3.10: SND configuration.

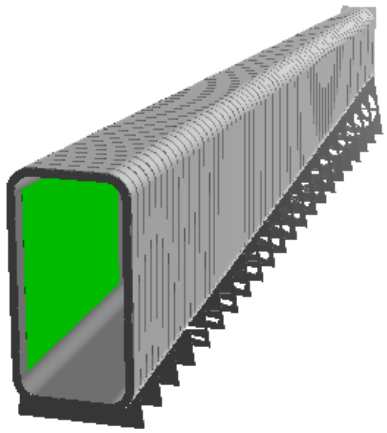

Figure 3.11: The vacuum vessel.

3.2.5 Decay Volume

Exploring hidden particles through direct detection of their decays costs a strong background rejection. A decay volume is there to provide the cleanest environment for decays from the hidden sector. The desired pressure inside the volume is 10^{-6} bar. Also, the vessel is surrounded by efficient background taggers not to take events from stray particles. The layout of the decay vessel is depicted in Figure 3.11.

3.2.6 Spectrometer and Calorimetry

The spectrometer consisting of 4 straw trackers and one dipole magnet- two tracking stations before the magnet, two after the magnet is devoted to make the momentum measurement and reconstruct the decay vertex. As far as the calorimetry is concerned, photons, electrons, pions must be identified to meet the requirements of the SHiP physics program. Therefore, both hadronic and electromagnetic calorimeters follow the spectrometer. Finally, at the most downstream of the SHiP setup, a muon identification system is located to identify muons coming from the vacuum vessel.

3.3 The SHiP Software: FairShip

FairShip is the software framework devoted to the provide environment for the simulation, event reconstruction and data analysis studies for physics searches. FairShip software framework is based on FairRoot [14] that combines ROOT [15] which is data analysis framework widely used at CERN, GEANT4 [16], a toolkit of the simulation of passage of particles through matter and event generators such as PYTHI6 [17], PYTHI8[18], and GENIE [19]. FairShip includes a branch dedicated to muon flux test beam through which studies in this thesis were conducted. The software is still very young and gradually evolving as response to evolution of SHiP.

CHAPTER 4

MEASUREMENT OF MUON FLUX FOR SHIP

One of important information needed for SHiP's meausurements is the flux and spectrum of muons emanating from the SHiP target. Motivating from this, a test beam measurement was done by impinging 400 GeV protons on a replica of the SHiP target at H4 beamline in the Perevessin site at CERN in 2018. We have fully participated in this test beam as the METU SHiP team. After three weeks of data taking the data has been rebuilt and reconstructed. The analysis of the collected data was completed and the results on muon flux have been published[11]. Further analysis on J/ψ production is going on, and is planned to be finalized within this year.

4.1 Experimental Setup

The muon flux spectrometer as shown in Figure 4.1 was installed as follows:

Two beam counters were placed in front of the target station to record POT. A 2.4 m hadron absorber made of iron followed the target. The target and absorber area were shielded by concrete walls. The hadron absorber was optimized to stop pions and kaons but still have p_T acceptance for muons. Four tracking stations (T1, T2, T3, T4) consisting of drift tube modules, a modified version from OPERA [12], were placed at the downstream of the absorber. T1 and T2 were upstream, T3 and T4 were downstream of the Goliath magnet. While two modules from T1 and T2 stations made a stereo setup i.e. T1 has both x,u views and T2 has both x,v views where u and v are planes 60° stereo angle in between. T3 and T4 had x views only. Stereo structures of x, u, and v planes are illustrated in Figure 4.2

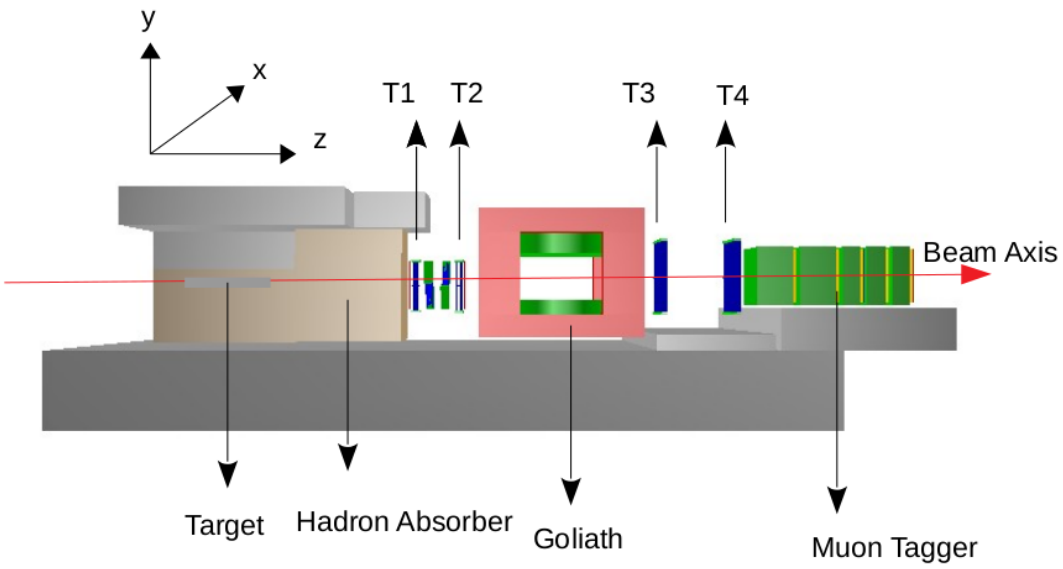

Figure 4.1: The spectrometer layout and the coordinate system as implemented in the FairShip.

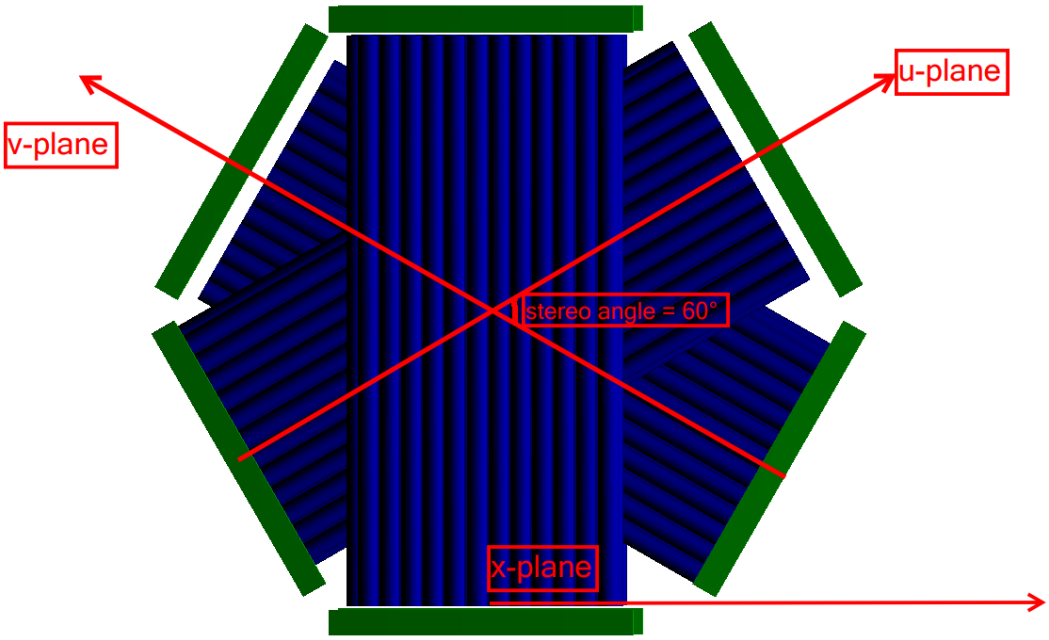

Figure 4.2: The stereo structure of modules of T1 and T2.

Tracking stations were followed by a muon tagger. The muon tagger was a combination of 5 stations of Resistive Plate Chambers (RPC) and iron slabs. Each chamber was separated by iron slabs, starting with the passive material. The RPC had both x

and y views. The alignment of the detectors was done by the CERN survey team up to a presicion of $\sim$ 5 mm [20]. The results were implemented in the FairShip software.

4.1.1 The Target

The target used in the test beam was a replica of the SHiP target. The detailed description of the target is given in Chapter 3. The replica of the target was a cylinder of 154.3 cm length and 10 cm in diameter.

4.1.2 The Hadron Absorber

The duty of the hadron absorber is to stop traversing hadrons such as Kaons and Pions. It's made of iron blocks making a volume of $240 \times 240 \times 240\ cm^3$.

4.1.3 Drift tubes

Drifttubes are typical proportional chambers widely used in high energy physics experiments as tracking detectors. The idea of detection in proportional chambers relies on the phenomenon known as gas multiplication. The gas multiplication can be considered as an avalanche of electrons of ionized gas atoms as the charged particle traverse through the gas. According to the celebrated Bethe-Bloch formula [3] the energy loss of the particle during its voyage in a medium is given as :

$$-\frac{dE}{dx} = Kz^2\frac{Z}{A}\frac{1}{\beta^2}\left[\frac{1}{2}ln\left(\frac{2m_ec^2\beta^2\gamma^2T_{max}}{I^2}\right) - \beta^2 - \frac{\delta(\beta\gamma)}{2}\right] \tag{4.1}$$

In this equation, ingridients are defined as

- $K = \pi N_A r_e^2 m_e$, r_e is the classical electron radius and N_A is the Avogadro number
- z : the electic charge of the incident particle
- m_e : the electron mass

- Z and A : the atomic and mass number of the container medium respectively
- β : particle's velocity in units of speed of light
- γ : the relativistic gamma factor
- T_{max} : the maximum kinetic energy that can be transferred to a free electron in a single collision by a particle of mass M
- I : the mean excitation potential of the target atom
- N_A: The Avagodro number
- $\delta(\beta\gamma)$: a correction factor due to denstiy effect

Energy loss of some particles through several media according to Bethe-Bloch formula is shown in Figure 4.3.

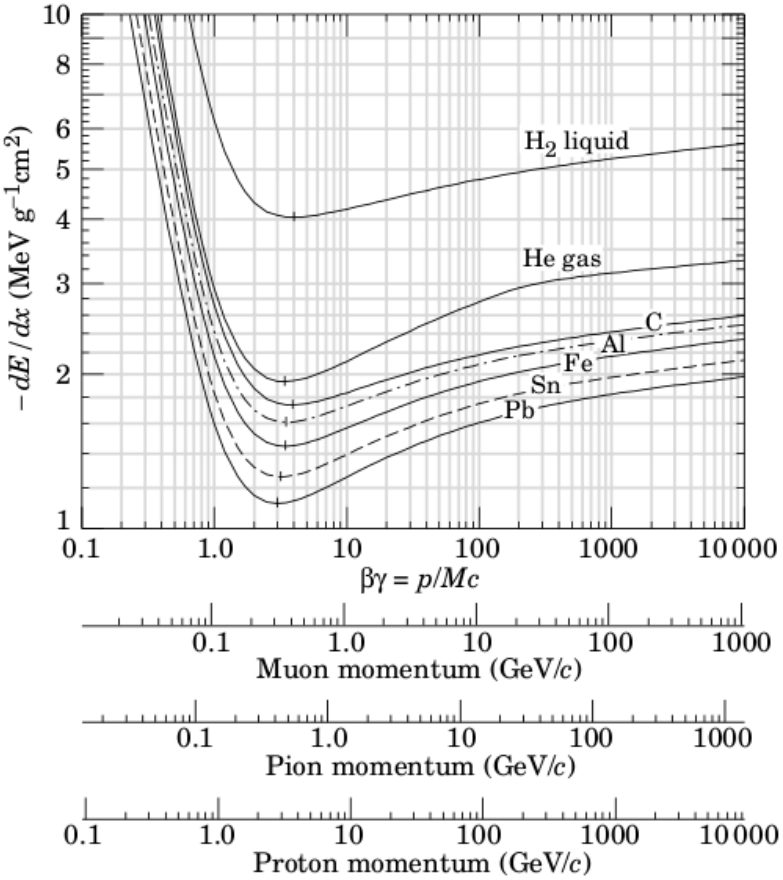

Figure 4.3: Energy loss of particles in several media.[3]

In order to form the avalanche, a strong electric field through a high voltage wire is applied inside the gas-filled detector. Charged particles lose energy as they traverse inside the gas through ionization or atomic excitation. The strong electric field inside the gas accelarates the liberated electrons of ionized gas through the wire. As a result of this, more and more electron electrons will be ejected. As ions are much heavier than electrons and thus their mobility is low, they won't contribute to this. The avalanche is finished when all electrons are collected by the wire providing a measurable electrical signal. The formation of avelanche is presented Figure 4.4.

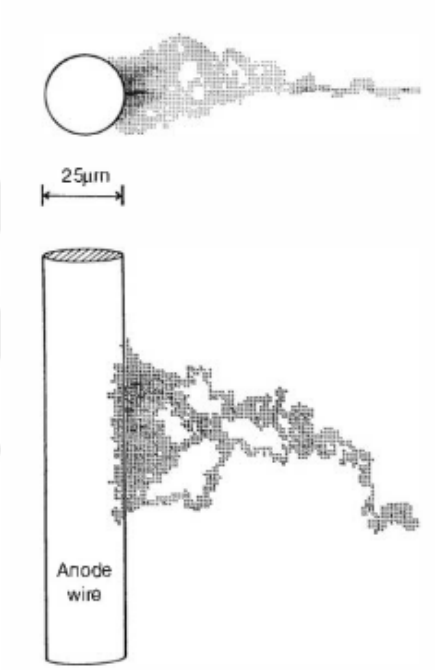

Figure 4.4: Illustration of avelanche formation.[3]

Using this method, drit tubes measure the drif time of electrons drifted inside the gas. To achieve this, another external trigger is necessary as a clock. The time difference between the trigger signal and the drifttube signal gives the drift time. Since the particle of the interest is assumed to be very fast, the delaying effect between two signals can be neglected. The radial position of the track with respect to the tube center (r) can then be determined after a calibration.

4.1.3.1 $r - t$ Calibration

For a track to be reconstructed the only r is of interest. In fact, drift tubes don't provide the true drift time but a digitized one (TDC). But this does not block the measurement of the r up to a certain precision as the r is directly related to TDC. The spatial resolution was expected to be 270 μm but it was measured as 350μm. An example of TDC distribution for three spills is presented in Figure 4.5. The peak corresponds to hits near the wire and the tail corresponds to hits near the tube wall. The entire spectrum can then be scaled to drift radii.

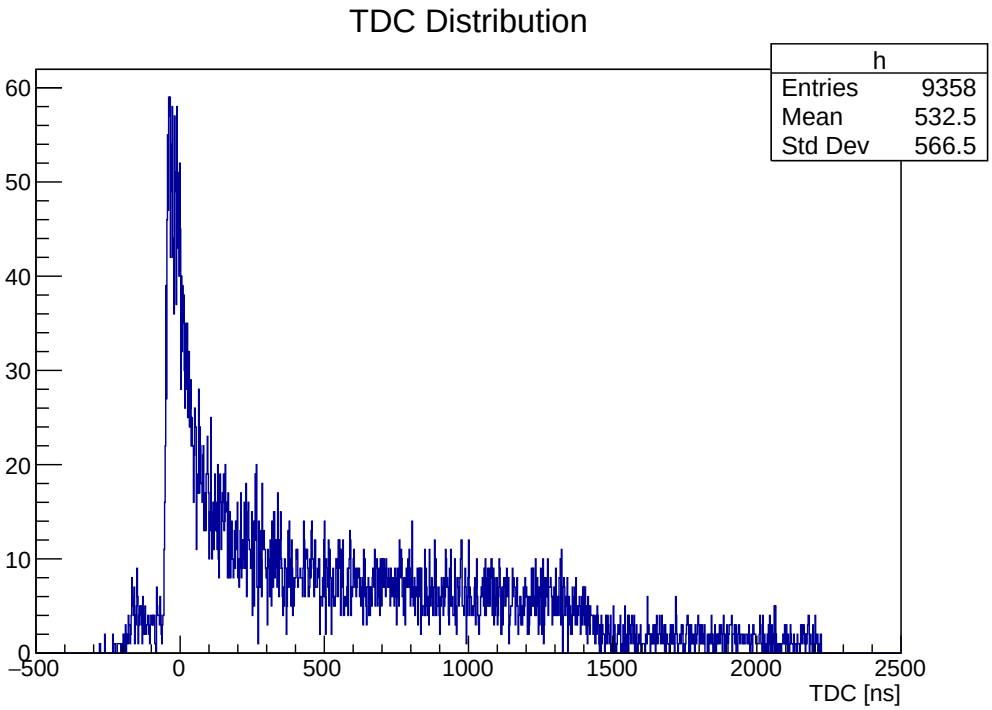

Figure 4.5: A TDC distribution of group of 12 channels of T4

The initial calibration to obtain the $r - t$ relation is done using the TDC spectrum of homogeneously illumuinated drift tube. As all drift radii are equally probable, for a given TDC, $r - t$ relation is obtained from the formula [21]

$$r(t_c) = r_{max} \frac{\sum_{i=t_c}^{N_{channels}} N_i}{\sum_{i=0}^{N_{channels}} N_i} = r_{max} \frac{\sum_{i=t_c}^{N_{channels}} N_i}{N_{Entries}} \tag{4.2}$$

Here r_{max} is 1.815 cm as it is the radius of a single tube. An example of $r-t$ relations

for $\sim 3-4$ spills is shown in Figure 4.6

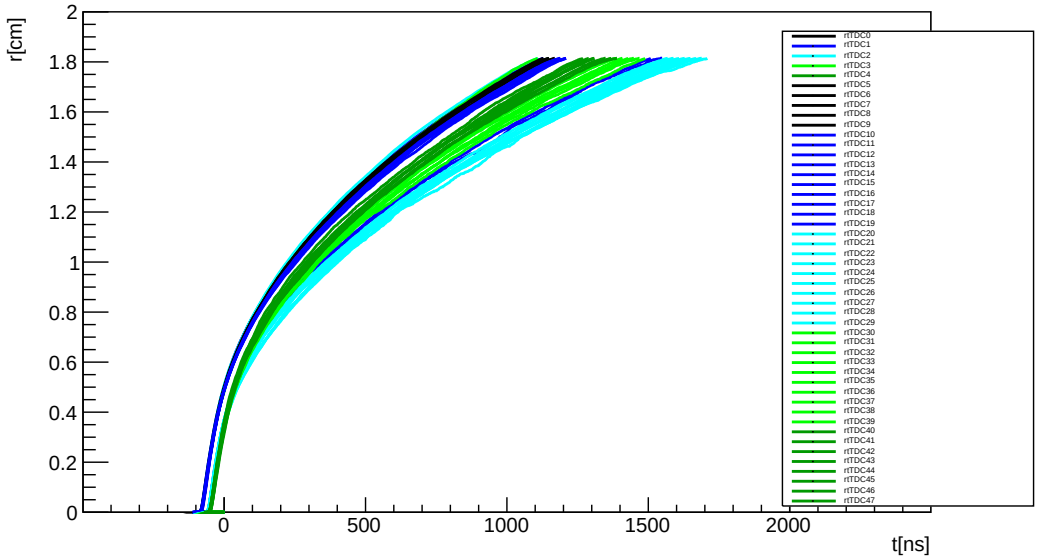

Figure 4.6: RT relations

4.1.4 Resistive Plate Chambers (RPC)

Unlike drift tubes, in RPCs no high voltage wire is used inside the gas. Instead, the space between two higly resistive plate is filled with a gas. Plates are induced with elecric field. This will make the detector to act like a capacitor. As the charged particle traverse through RPC planes it causes a local discharge on resistive plates which induce signal in the readout strips, and are made of bakelites. Signal formation in RPC is illustrated in Figure 4.7 This structure of RPCs makes them very fast. They

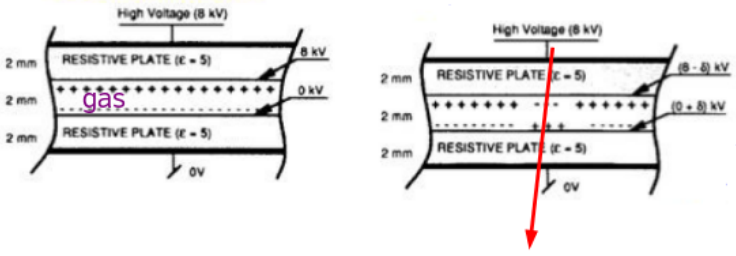

Figure 4.7: Illustration of signal formation in RPC.

are therefore widely used in experiments with high event rates. In the test beam, the

Table 4.1: Three different magnetic field configurations.

Field	Goliath Current	David Current
Nominal	3600 A	1600 A
Intermediate	2400 A	1166 A
Zero	0 A	0 A

Table 4.2: Data taken with three different fields.

Field	raw proton counts	number of spills
Nominal	2.81×10^{11}	20128
Intermediate	2.4×10^{10}	1552
Zero	2.3×10^{10}	1445

muon tagger was consist of five RPCs layers each interleaved by iron blocks.

4.2 Data

During the three weeks of data taking period ~ 20 k spills yielding 2.81×10^{11} raw proton counts, not normalized, were recorded with the nominal magnetic field. In addition to this, data has been taken with two other magnetic field configurations i.e. an intermediate field with lower currents in the Goliath coils and zero field. To calculate the POT delivered, one must take the different dead times and widths of scintillators. Moreover, some protons, the so-called halo protons must also be taken into account. According to this normalization, our dataset with the nominal field corresponds to $(3.25 \pm 0.007) \times 10^{11}$ POT [22]. The number of POT per μ event at which at least one muon is reconstructed is 710 $\pm$ 15 for the nominal field and 625 $\pm$ 15 [22] for the intermediate field. The intermediate field has a higher rate of reconstructed muons simply beacause the lower p_T kick by the magnetic field increases the acceptance of detectors. Magnetic field configurations with respect to currents in magnet coils and raw proton counts are tabulated in Table 4.1 and Table 4.2, respectively.

4.3 The Momentum Measurement

The task of the spectrometer is to measure the momenta of charged particles emanating from the hadron absorber. This is done by exploiting the deflection given by the magnet as a result of the Lorentz force.

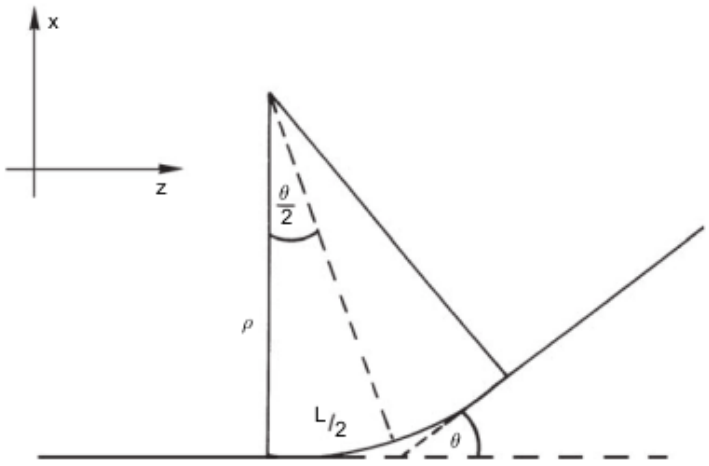

Figure 4.8: Illustration of trajectory of a charged particle in a magnet. Figure adapted from the reference. [3]

Let's presume the magnetic field $\vec{B}$ is oriented along the y axis i.e. $\vec{B} = (0, B_y, 0)$ and the particle enters to the magnetic field along the z axis. This leads the deflection of charged particles to be in the xz plane. For a particle traveling along the z axis $|\vec{p}| = p_z$ where $\vec{p}$ is the momentum vector and p_z is its longitudinal component. Then, the centripetal force due to the Lorentz force

$$\frac{mv^2}{\rho} = qvB_y \tag{4.3}$$

where m is the mass, v is the velocity, q is the charge of the incident particle and ρ is the bending radius. Then, ρ can be obtained immediately from Equation 4.3 as

$$\rho = \frac{p}{qB_y} \tag{4.4}$$

With the standart units commonly used in particle physics Equation 4.4 becomes

$$\rho[m] = \frac{p[GeV/c]}{0.3B[T]} \tag{4.5}$$

The bending radius ρ is generally very large compared to the length of the magnet i.e. $\rho >> L$. Then, we can approximate the deflection angle θ as

$$\theta = \frac{L}{\rho} = \frac{L}{p} q B_y \tag{4.6}$$

The magnetic deflection leads to a kick in the transverse momentum of the charged particle. This additional transverse momentum can be estimated from the geometry as shown in Figure 4.8. The change in the transverse momentum Δp_x, on the other hand

$$\Delta p_x = p \sin\theta \approx p\theta \tag{4.7}$$

Combining Equation 4.6 and Equation 4.7 we get

$$\Delta p_x = L q B_y \tag{4.8}$$

Equation 4.8 is for the uniform B_y. For the varying field along the magnet Equation 4.8 transforms to

$$\Delta p_x = q \int B_y dl \tag{4.9}$$

In order to understand the geometric acceptence of muon flux detectors one must take the deflection given by the magnet into account. There is a maximum deflection angle θ_{max} accepted by T3 and T4. This θ_{max} can be extraced from the slope of the line joining the centre of the Goliath and the position of the outermost tube of T3. This is illustrated in Figure 4.9.

In terms of momentum there is a minimum momentum to make a hit at T3 and T4. The slope of the track after the magnet, $\Delta p_x/p_z$, should be less than θ_{max}. Since

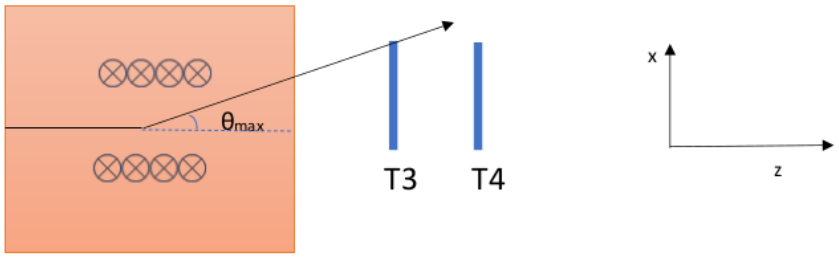

Figure 4.9: Illustration of maximum deflection angle

the kick, Δp_x, is the same for every track, the particle require a momentum above a certain value.

The minimum momentum required can be estimated using the deflection given by magnetic field. The task here is to calculate the $\int BdL$ of the magnet. This can be achieved using the field map [22] as shown in Figure 4.10 and Figure 4.11. Then, using Equation 4.9, Δp_x can be estimated.

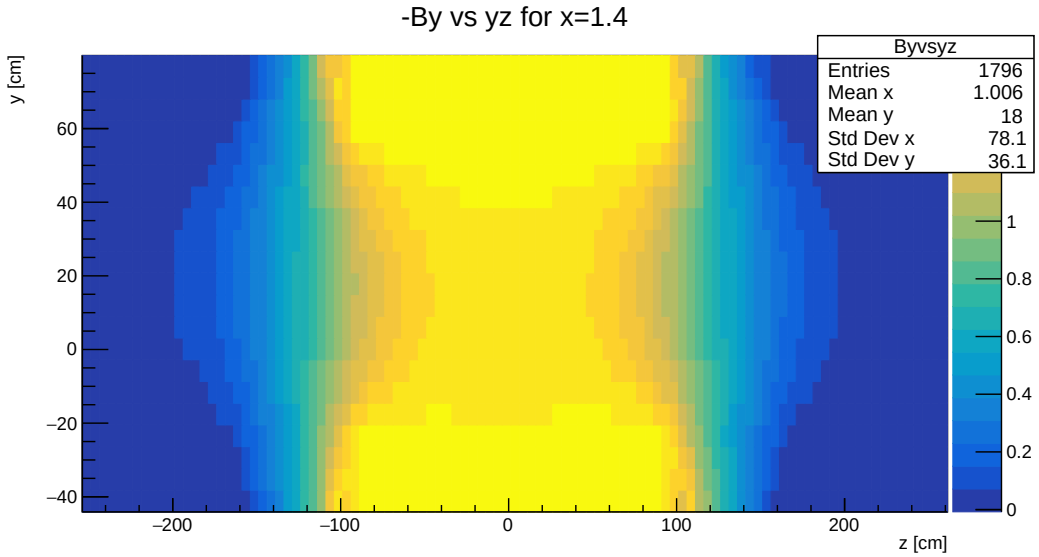

Figure 4.10: The B_y component as a function of y and z at $x = 1.4m$ with respect to the center of Goliath.

Assuming the particle enters to the magnetic field through along the beam axis, the slice at x=0. y=0. of the B_y vs z of the map can be used.

Since this map is a histogram object in ROOT, the integral can be carried out by

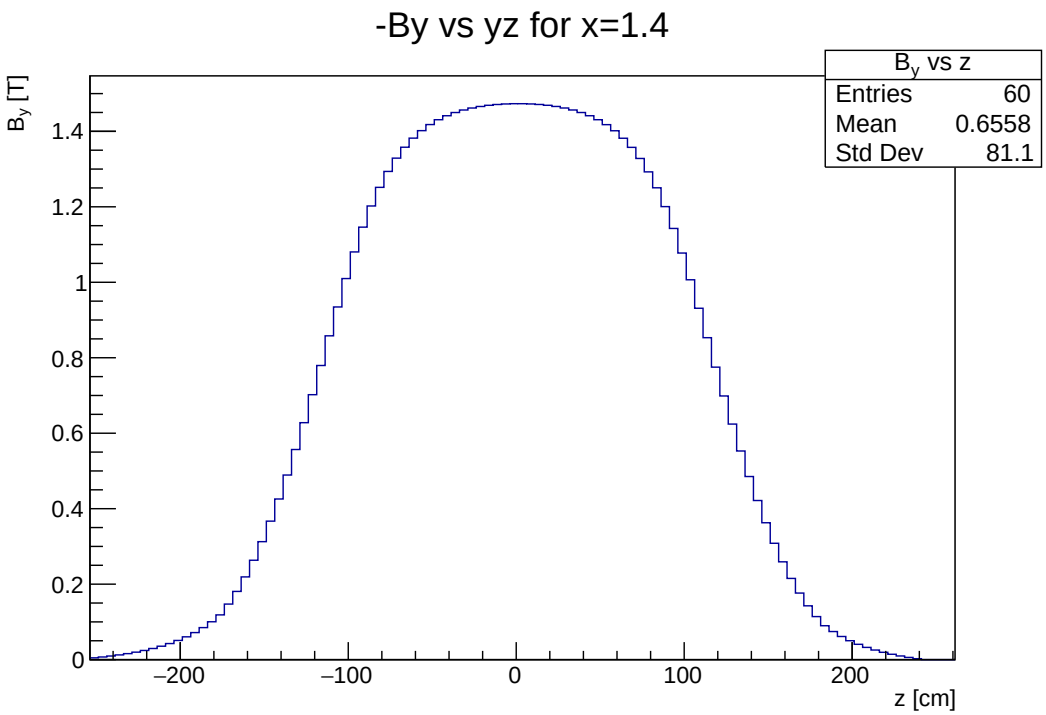

Figure 4.11: B_y as a function of z at x=1.4 m, y=0. in the Goliath reference frame.

ROOT. Putting all these together, a minimum momentum of 2.5 GeV/c is required to pass through T3, and 4 GeV/c is for T4.

The nominal value of the spatial resolution of the spectrometer was 270 μm but it is measured as 350 μm in the data. The momentum resolution of muon flux spectrometer as a function of momentum for two values of spatial resolution is shown in Figure 4.12. It's seen how reduced hit precision degrades the precison of the momentum measurement. At low momenta the momentum resolution is affected by the multiple scattering [22].

4.4 Track Reconstruction

The procedure of the reconstruction consists of two steps [22]:

- Make RT relations using 3-4 spills (for number of events > 350.000) for the data. This is not needed for MC. This is obtained by simulating the drift radius with the nominal resolution for the MC.

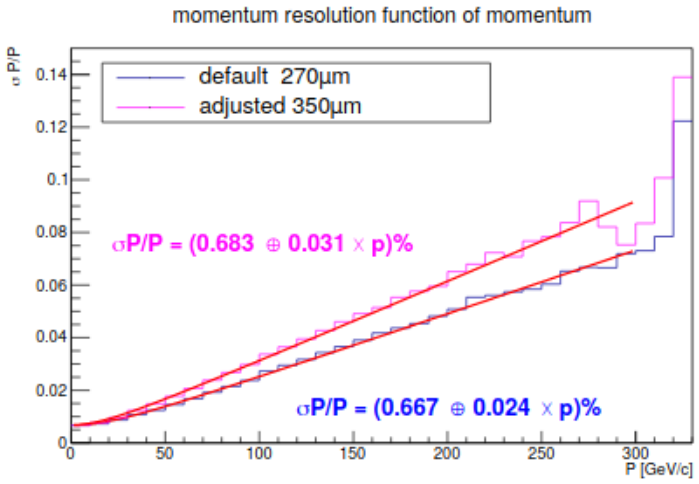

Figure 4.12: The momentum resolution as function of momentum for two values of spatial resolution.

- Find track candidates with a pattern recognition algorithm first. Then, fit tracks using the RT relations.

The pattern recognition searches for track candidates by forming clusters of hits across drift tube modules and combining them into tracklets before and after the magnet. If these tracklets are sufficiently close at the center of the Goliath the combination is ascended to a fitted track. The track fit is performed with the GENFIT-"a Generic track-fitting toolkit" [23] package using an iterative Kalman filter. The trackfit takes the field map and material effects i.e. energy loss into account.

CHAPTER 5

SEARCH FOR $K_S^0 \rightarrow \pi^+\pi^-$ IN THE SHIP TEST BEAM DATA

The SHiP experiment is dedicated to search for the new physics in an environment as silent as possible. Therefore, background studies are very important for SHiP. Main sources of the background for the SHiP experiment can be itemized as follows:

- Muon or neutrino induced background: muons or neutrinos that escape from the target could interact with the surrounding medium of the decay volume and produce V0 particles that could induce a similar signal with the HS signal.
- Combinatorial background: Two random tracks could simultaneously enter the decay volume and produce a fake vertex that resembles to the SHiP signal.
- Cosmic muons: Stray muons coming from the atmosphere could induce a fake signal.

Among V0 particles, especially, neutral kaons are very dangerous since the majority of the background comes from the decays of neutral kaons as presented in Table 5.1

The precision measurements for neutral kaons have been done by NA62/48 experiments at CERN over decades [24] [25]. Therefore, branching ratios and the mass of K_S^0 are well established.

The muon flux test beam setup has provided a chance to study muon induced V0 events. In this thesis, the $K_S^0 \rightarrow \pi^+\pi^-$ event was studied. The lack of particle identification in the test beam setup does not permit us to study others such as Λ and K_L^0 decays.

Signal	SHiP Phiscs	Background
$\pi^+\pi^-$	DP, PNGB,HP	$K_L^0 \to \pi^+\pi^-\pi^0$ $K_L^0 \to \pi^+\pi^-$
$\pi^+\pi^- p^{miss}$	DP, PNGB, HP, HNL	$K_L^0 \to \pi^+\pi^-\pi^0$ $K_L^0 \to \pi^+\pi^-$ $K_S^0 \to \pi^+\pi^-$ $\Lambda \to p\pi$
K^+K^-	DP, PNGB, HP	$K_S^0 \to \pi^+\pi^-$ $K_L^0 \to \pi^+\pi^-$ $\Lambda \to p\pi$

Table 5.1: Table showing the signal and background channels. DP = Dark Photon, HNL = Heavy Neutral Lepton, PNGB= Pseudo-Nambu Goldston Boson, HP= Higgs Portal.

5.1 MC Simulation with Muon Deep Inelastic Scattering

Muons could scatter-off the nuclei and produce hadrons. Pions, kaons, and other particles such as Λ baryons are emitted from such events. If this happens in last few centimeters of the iron absorber of the muon flux setup, (about one nuclear interaction length of the iron $\sim$ 17 cm) these muon induced hadrons would be detected through their decays. As far as the K_S^0 decays are concerned, having two pion in the final state makes the decay topology unique and simple. The diagram in Figure 5.1 represents a muon DIS event.

The production of K_S^0 has been simulated with PYTHIA6 muon deep inelastic scattering (DIS). Since the hadron absorber stops traversing hadrons produced inside the target, we are interested in events occurring near the end of the hadron absorber. Therefore the standalone K_S^0 production was done 10 cm before the absorber. On the other hand, in order to estimate the number of particles leaving the hadron absorber per spill, another simulation using the FixTarget event generator that generates events starting proton interactions in the target was done. The number of events in this simulation corresponds to one spill, that is, $\sim 17 - 18$ M POT. In this simulation, despite

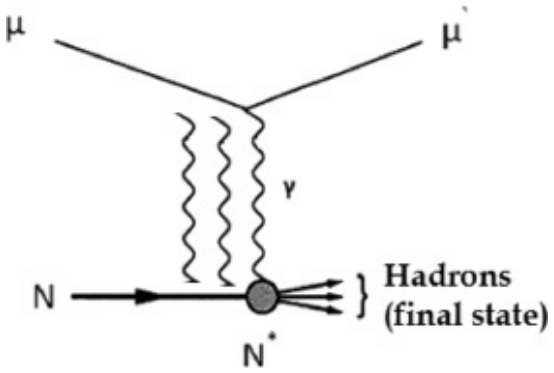

Figure 5.1: The diagram showing the muon deep inelastic scattering. [4]

several K_S^0s leave the absorber, we had no $K_S^0 \to \pi^+\pi^-$ induced signal. Therefore, we will be focusing on the production through muon DIS.

The procedure for the muon DIS simulation is as follows:

- Produce primary DIS events with PYTHIA6 and record these events. The outputs are particle IDs, momenta, and weights of generated particles. Use muons from the 2018 muon background simulation as input muons.
- Feed these events to GEANT4, splattering them uniformly over the downstream of the hadron absorber and let them decay, observe how detectors respond to these events.

True momentum distributions of input muons and outgoing kaons are presented in Figure 5.2 and Figure 5.3 respectively. The flight length distribution obtained from GEANT4 is shown Figure 5.4 showing that they could induce a signal in the test beam if vertices are just before the tracking stations. An example of $K_S^0 \to \pi^+\pi^-$ event taken the event display is shown in Figure 5.5

5.1.1 Number of Expected DIS Events

The expected number of muon DIS events can be estimated using [1]

$$N_{DIS} = \frac{\int N_\mu \sigma_{DIS}(p) N_{spills} \rho_{material} l \phi(p) dp d\Omega}{\int \phi(p) dp d\Omega} \tag{5.1}$$

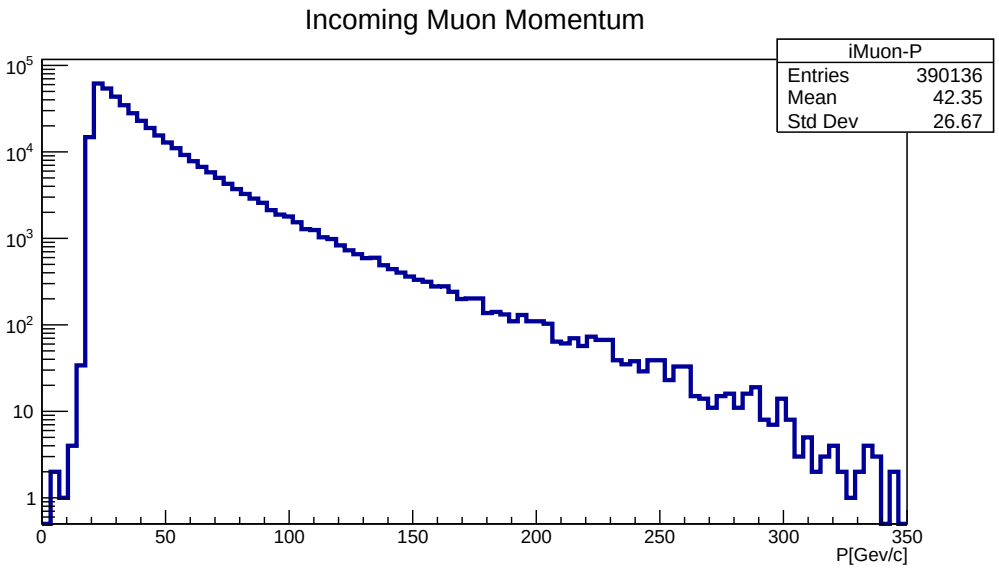

Figure 5.2: The momentum distribution of muons used as input in the DIS simulation.

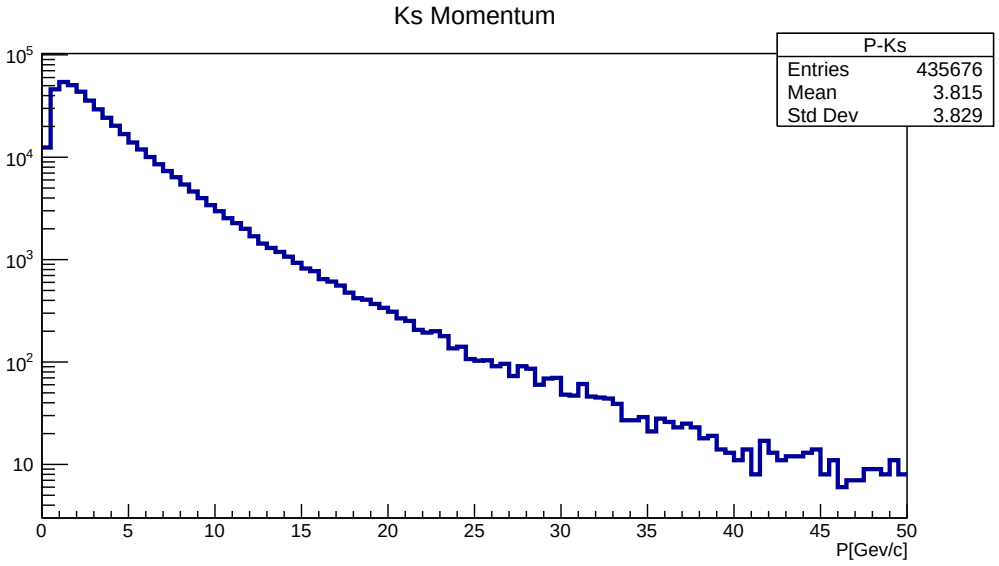

Figure 5.3: The momentum distribution of K_S^0 from PYTHIA6.

Here N_μ is the number of incoming muons per spill. σ_{DIS} is the cross- section taken from [26], N_{spills} is the total number of spills. The factor $N_\mu \cdot N_{spills}$ can be adapted from the normalization as 4.6×10^8. $\rho_{material}$ is the mass density of the material in which the DIS event occurs. This is $7.874t/m^3$ for the iron. l is the length of the material. We have located K_S^0 events over the last 10 cm of the hadron absorber. Since in the deeper regions, K_S^0 or its daughters are expected to be stopped by the

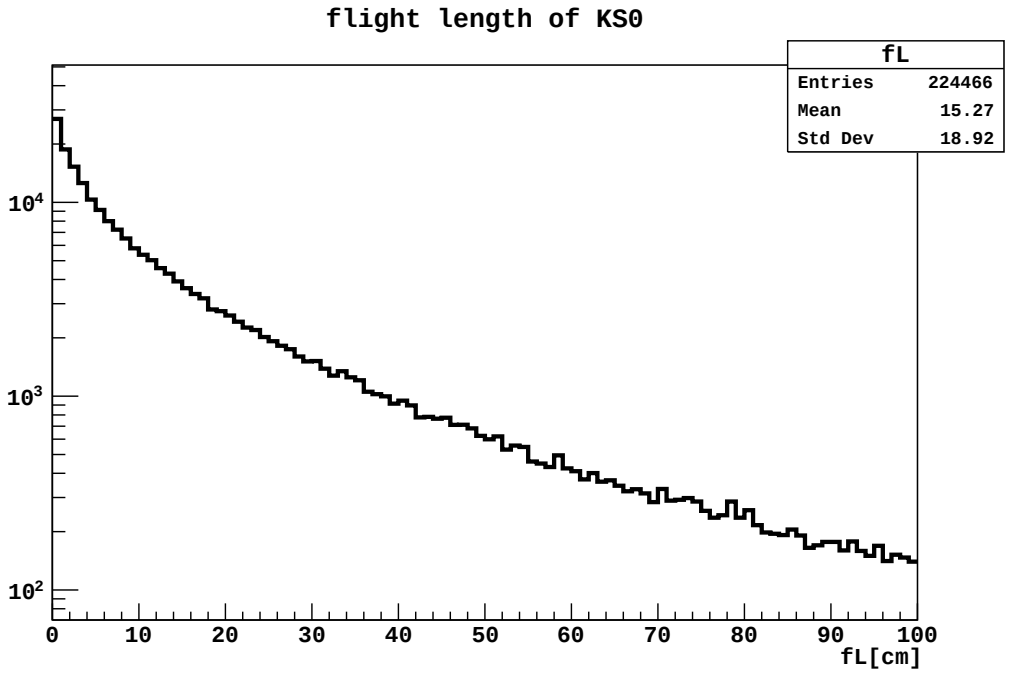

Figure 5.4: The flight length distribution of K_S^0.

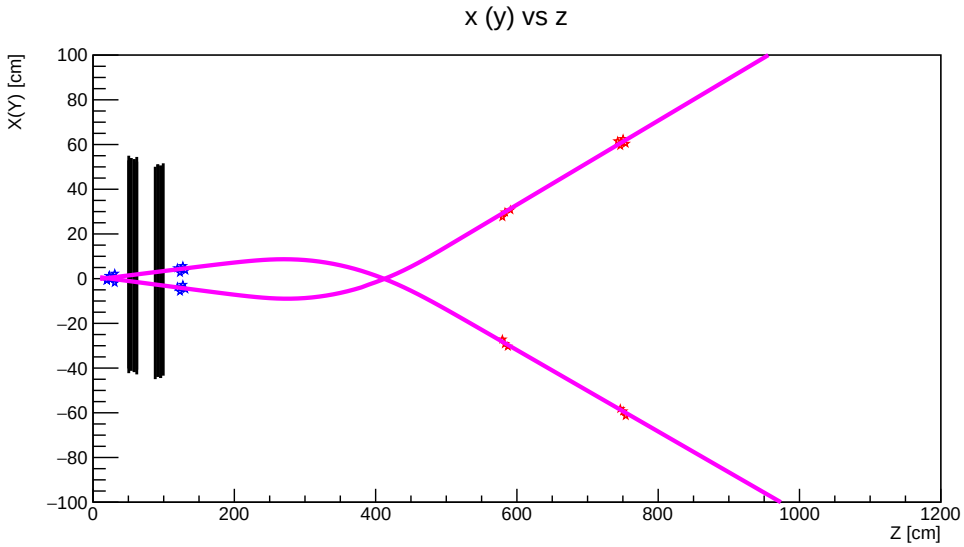

Figure 5.5: A $K_S^0 \to \pi^+\pi^-$ event in the event display.

iron. The last ingredient $\phi(p)$ in this is the momentum spectrum of muons. This can be extracted from either data or MC. Putting all these together, the number of DIS events inside the last 10 cm of the hadron absorber is estimated as $\sim$ 20k.

5.1.2 K_S^0 Kinematics

The reconstructed K_S^0 events have been analyzed for both nominal and intermediate fields.

5.1.2.1 Armenteros-Podolanski Distribution

The Armenteros-Podolanski distribution is very useful in particle identification. It's motivated from the symmetry in the momenta of the decay subproducts. It's the correlation of the parameter q_T and the parameter α which are defined as [27]:

$$\alpha = \frac{p_l^+ - p_l^-}{p_l^+ + p_l^-} \tag{5.2}$$

where $p_l^{+(-)}$ is the longitudinal component of the positively (negatively) charged track. q_T is the transverse momentum of the positively charged particle.

The Armenteros-Podolanski distribution obtained from true pion tracks is presented in Figure 5.6.

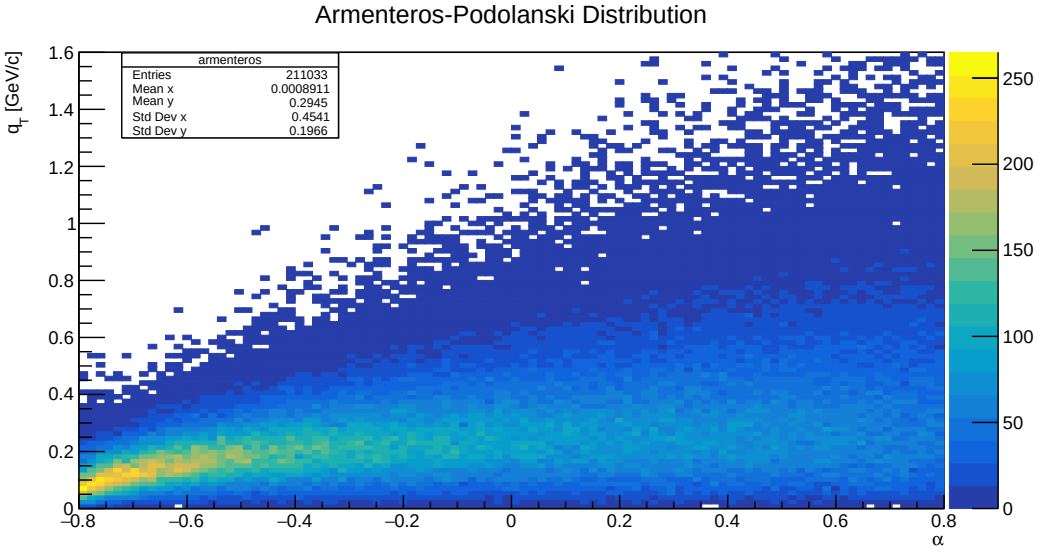

Figure 5.6: The Armenteros-Podolanski distribution of MC $K_S^0 \to \pi^+\pi^-$ events.

5.1.3 Invariant K_S^0 Mass

The main decay mode of the K_0^S is the $\pi^+\pi^-$ mode ($\Gamma_{\pi^+\pi^-}$ / Γ= 69.20 %).

The invariant K_0^S mass from two pions with masses m and four-momenta p_1 and p_2 can be calculated from Lorentz Invariance

$$M_{K_0^S} = \sqrt{2 \cdot m^2 + \sqrt{(m^2 + \mathbf{p_1}^2) \cdot (m^2 + \mathbf{p_2}^2) - \mathbf{p_1} \cdot \mathbf{p_2}}} \tag{5.3}$$

We had applied this to the MC and data using the distance of closest approach (doca). We had observed a very low mass peak that is due to wrongly reconstructed vertices i.e. very close tracks results in shared hits in the first detector plane, plus a peak around the K_S^0 nominal mass (497.611 $\pm$ 0.013) as shown in Figure 5.10. This very low mass peak can be understood by plotting the vertex position versus the invariant mass. The plot in Figure 5.7 shows that the majority of these wrongly reconstructed vertices are cumulated around $z \sim 50$ cm. This is the midpoint of the T1 station where hits shared by two tracks are cumulated. The true and reconstructed vertex positions of K_S^0 decays are presented in Figure 5.8. The minimum distance between two tracks from K_S^0 decays is presented in Figure 5.9.

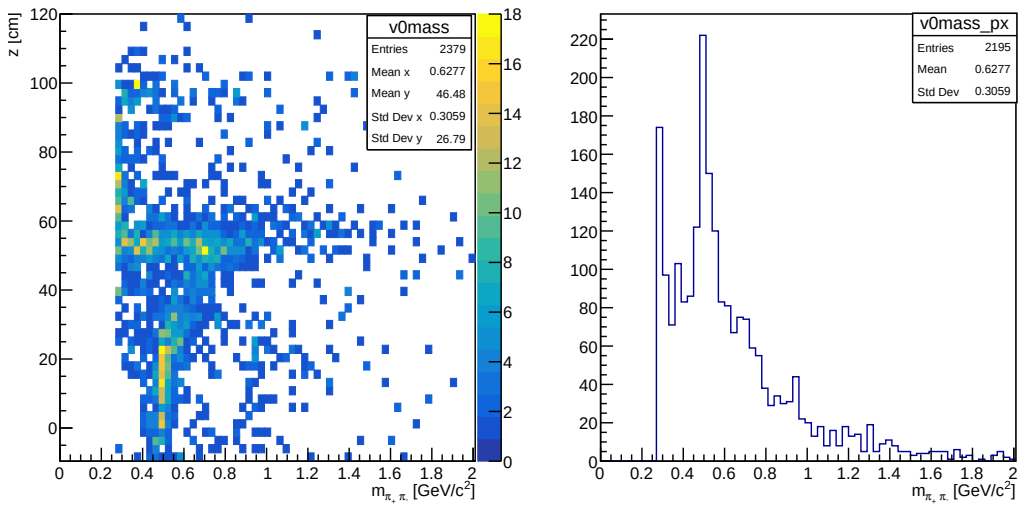

Figure 5.7: Left: Invariant mass vs. vertex position. Right: Invariant mass. Incorrect vertices can be seen.

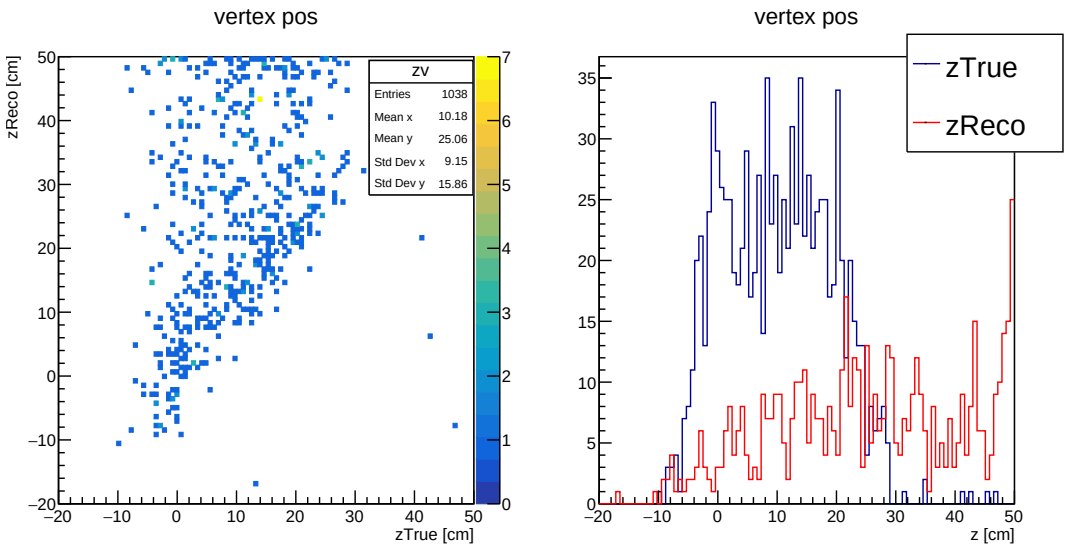

Figure 5.8: Reco vs. True vertex positions.

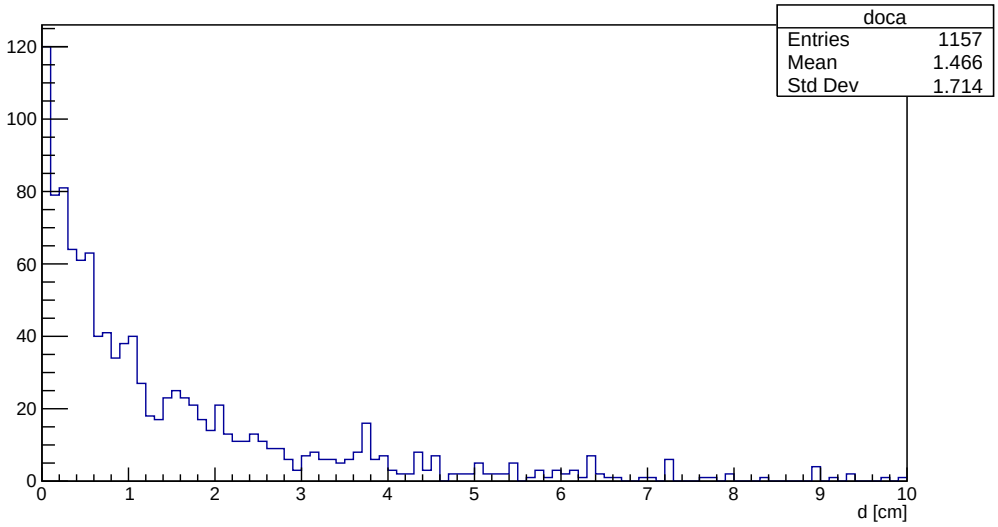

Figure 5.9: The minimum distance between two tracks from K_S^0 decays.

It is also observed that the number of reconstructed K_S^0 vertices is very low. In the muon DIS simulation, $\sim$ 220k $K_S^0 \rightarrow \pi^+\pi^-$ was produced, but the number of reconstructed events is just above two thousand for the nominal field. In the following sections, this inefficiency is explained in detail.

The analysis described above has been done over K_S^0 standalone production i.e. all other subproducts of the DIS event were switched off. The majority of subproducts,

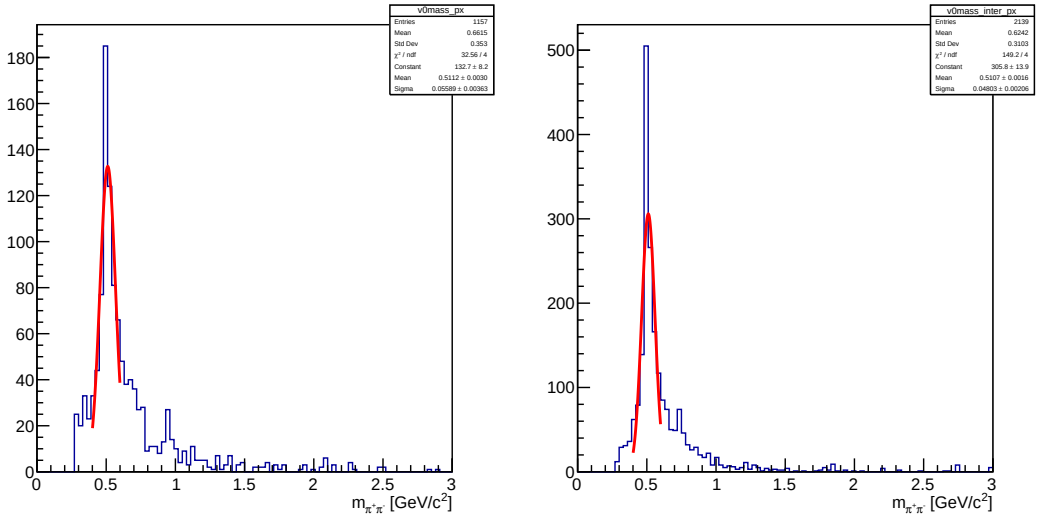

Figure 5.10: Invariant K_S^0 mass for MC. Left: nominal field, right: intermediate field. The number of reconstructed events is larger for the intermediate field.

in fact, were pions in the simulation. The task here is then to classify events with more than one pion track: those who are originated from K_S^0 or those from the direct production. In principle, this separation must be seen in the invariant mass because of the correlated production of the latter results in a different peak.

5.1.3.1 Aside : Muon DIS Full Simulation

As far as the full production of the muon DIS simulation is concerned, direct production of pions constitutes the main background for the K_S^0 signal. The production of events with more than one tracks yields another peak in the invariant mass as shown in Figure 5.11. Some selections are needed to distinguish K_S^0 events from other events with pions at final state. In order to tag K_S^0 decays, several kinematic and geometric parameters are studied in detail. One of the parameter we investigated is the so-called coplanarity angle of K_S^0 decays. However, since we don't know the incoming K_S^0 direction in the data obtained from the testbeam, this is studied using the MC events only to show how good is the coplanarity angle reconstructed.

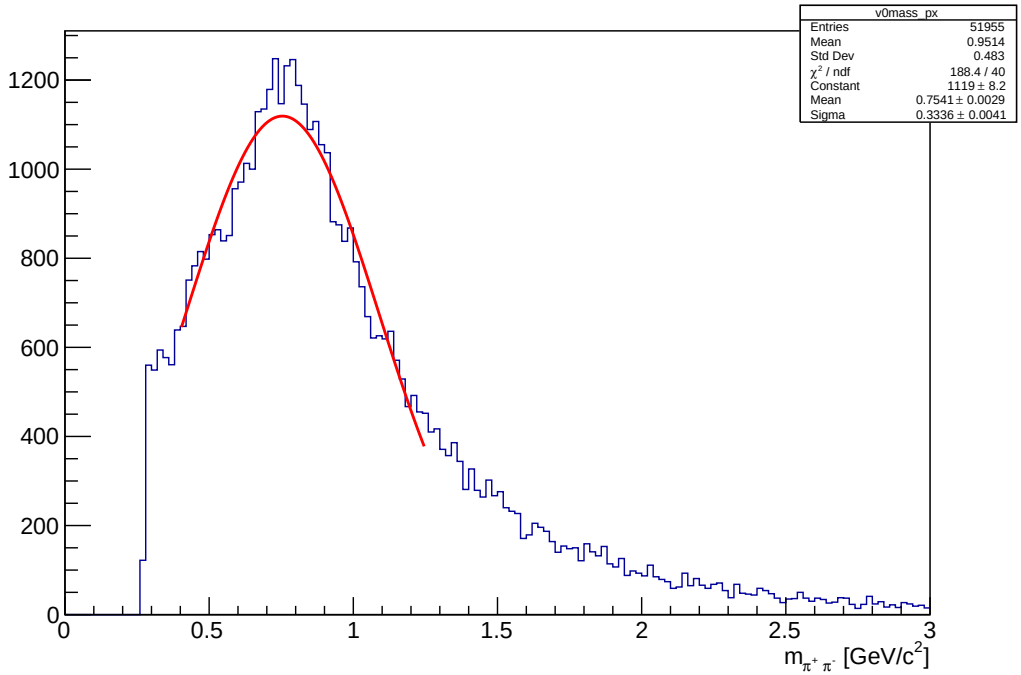

Figure 5.11: Invariant mass distribution of two pion events. The contribution from K_S^0 is not visible.

5.1.3.2 Coplanarity

Two body decays have their characteristic topology. First of all, in two body decays, the normal vector of the decay plane should be perpendicular to the incoming K_S^0 direction. The normal vector of the decay plane can be obtained from the cross product of pion direction. Then the angle between this vector and incoming K_S^0 direction will give the coplanarity angle, $\theta_{coplanarity}$. It is more convenient to define it as $\phi = \theta_{coplanarity}$-$\pi$/2. This is expected to be zero for $K_S^0 \rightarrow \pi^+\pi^-$ events. The distribution of coplanarity angle obtained from reconstructed tracks with respect to the true K_S^0 direction is shown in Figure 5.12.

Furthermore, pions must be back-to-back in the rest frame of the K_S^0. In the language of geometry, the projection of the momentum vectors should cancel each other in the transverse plane of incoming K_S^0.

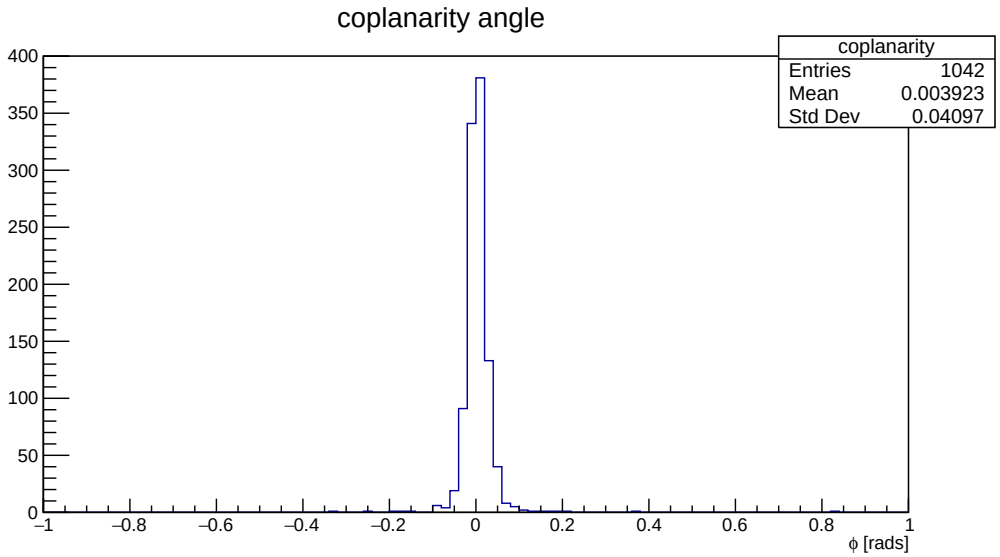

Figure 5.12: Coplanarity angle distribution. Reconstructed pion direction and true K_S^0 are used.

5.1.4 Reconstruction of Pion Tracks

It is well established that muons and pions have very similar dE/dx in the gas as shown in Figure 4.3. Therefore, pions passing through every four stations are expected to make hits and tracks must be reconstructed. Furthermore, pions live long enough to reach the last station. The comparison between true MC tracks and reconstructed tracks is shown in Figure 5.13.

However, a large number of pion tracks originated from K_S^0 produced by muon DIS cannot be seen by the spectrometer. The reason for that is low momentum K_S^0 do not give enough boost to its daughters to pass through the magnet and the magnetic field sweeps particles with momentum below ~ 4 GeV$/c$.

In order trace the loss in the reconstructed K_S^0 vertices, the tracking performance of the spectrometer has been studied. Since the reconstruction precedure requires at least two hits in each tracking station and each view [22], the number of hits per station must be known to track down the loss. This is tabulated in Table 5.2 for K_S^0 standalone production.

It can be understood from Table 5.2 that the vast majority of pions are lost after the

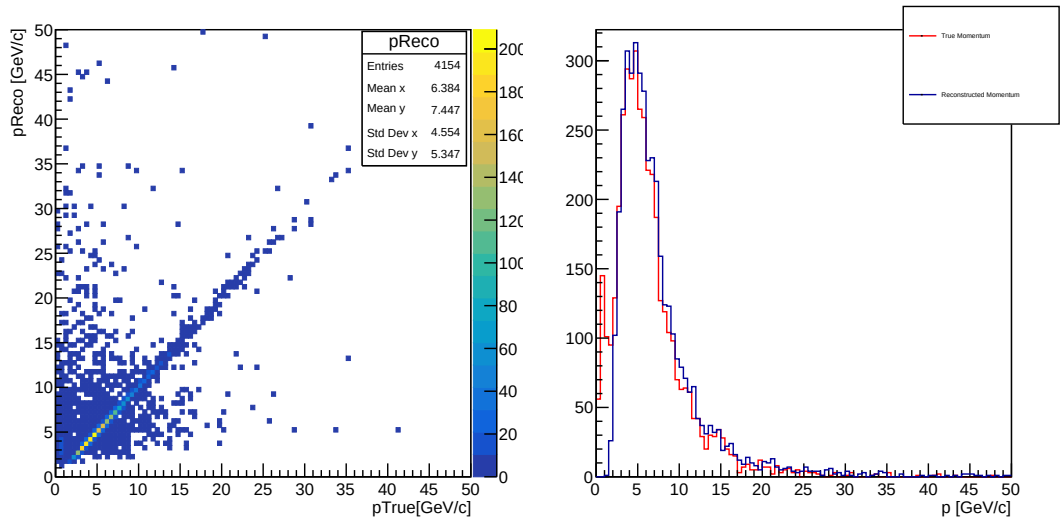

Figure 5.13: Reconstructed versus True momentum of pions from K_S^0 decays.

Total	T1x	T1u	T2v	T2x	T3	T4
448k	320k	320k	290k	260k	82k	47k

Table 5.2: The number of hits per each station due to $\sim$ 448k true pion tracks originated from K_S^0.

magnet. Furthermore, the true momentum distribution of pions just before the magnet is shown in Figure 5.14.

Furthermore, deflection and new x-positions of the pions after the magnet can be estimated from the p_T kick as explained in Chapter 4.

Putting these together, it is understood that the loss of the tracks is mainly due to their momenta that is, soft pions are swept out by the magnet.

5.1.5 Identification of Pions

In order to identify pions in the data the signature of pions at RPCs has been studied in detail. Layers of muon tagger start with the passive material first. Pions traversing through the iron are expected to make showers. However, the first passive layer can absorb all shower products below a certain energy. For a better understanding, another

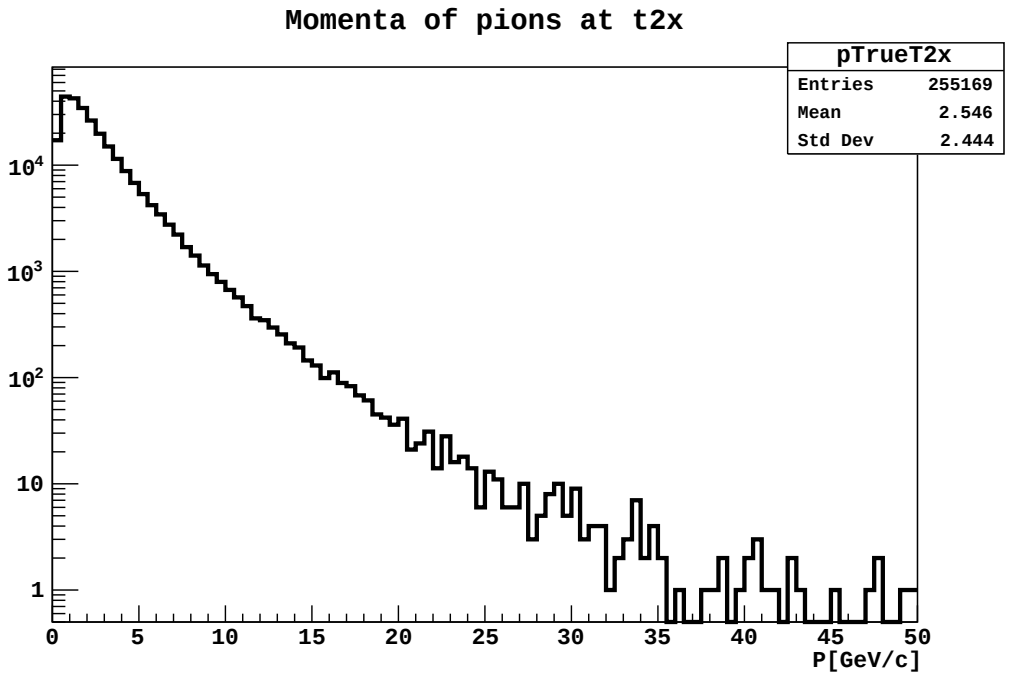

Figure 5.14: The true momentum distribution of pions before entering the magnet. i.e. the momentum at T2.

MC study has been carried out by shooting pions directly to the muon tagger. The pion beam in MC events have been processed through GEANT4 with zero field in which pions are impinging straight through on the iron. Then, the number of hits associated with the track per RPC station is counted. This is done by extrapolating tracks to RPC's active layers and look for hits that are close to tracks less than 10 cm. For muons, this study was done using the POT simulation. This study suggests that majority of pions having momenta less 50 GeV$/c$ will be stopped by the absorber leaving either no hit or occasionally few in the first RPC layer. Muons, on the other hand, can pierce through the iron blocks and make hits.

This convention has provided more than 99% correct seperation between muons and pions above 10 GeV$/c$ in muon DIS MC provided that extrapolated track is within the RPC acceptance. However, when we consider the POT MC which is the simulation starting from impinging 400 GeV protons on the target, the number of muon tracks dominates over number of pion tracks, our particle identification convention fails when seperating pions from muons. Momenta of pion candidates in the POT MC and the data are compared with the momentum of true pion tracks in the POT MC above

10 GeV/c. This is presented in Figure 5.15.

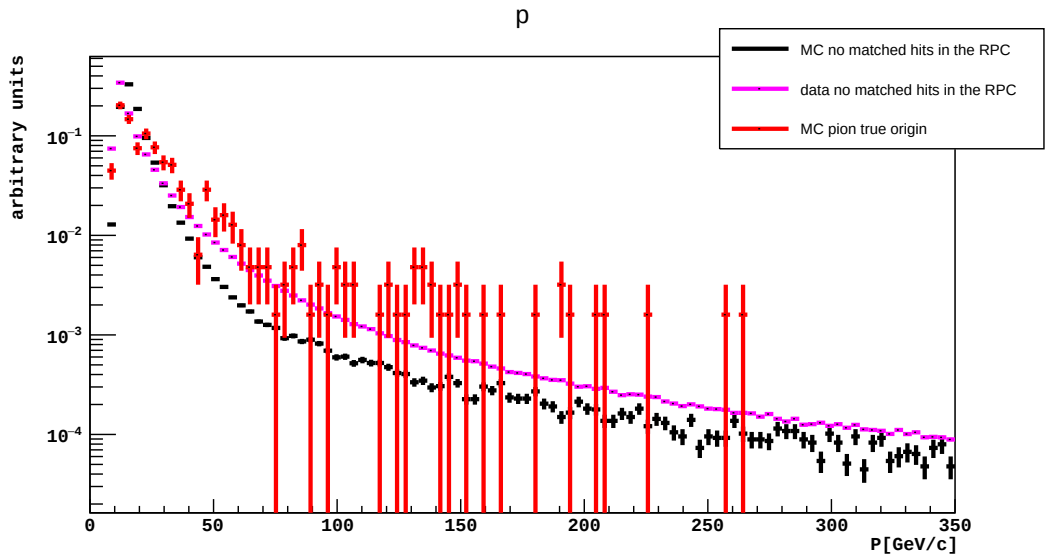

Figure 5.15: Momentum distributions of pion candidates in POT MC and data. The momentum distribution of true pion tracks is also shown.

This study suggests that we will be mixing muons and pions when we try to observe K^0_S signal in the data.

5.2 Data

After becoming familiar with K^0_S decays in the MC, the invariant mass of two pion events in the data is studied. In the data, in addition to muon DIS, other production mechanisms such as hadronic inelastic processes are involved. Furthermore, because the data is not clean as MC, background yield is expected to be more. Multiple scattering and the precision of particle identification might not also be omitted for the data. In the proceeding subsections, applying the pion track selection, the invariant mass study of two pion events is presented.

5.2.1 Track Selection

The test beam setup was not instrumented with a calorimeter. A muon tagger was installed for muon identification. However, following muons, the majority of particles

leaving the hadron absorber and making hits in drifttubes are expected to be pions. Origins of such tracks in the POT MC that we mentioned earlier is presented in Table 5.3. According to this simulation, no reconstructed track other than muon or pion is foreseen above 10 GeV/c. Combining this with our pion identification convention, plus several quality requirements can be compiled as:

$E_{kin} > E_{min}$	e^-	K^+	K^-	p	π^+	π^-	μ^+	μ^-
1 GeV/c	0.00	0.06	0.06	0.28	0.56	0.89	378.89	443.11
10 GeV/c	0.00	0.00	0.00	0.00	0.06	0.5	153.17	184.11

Table 5.3: Table showing the origins of tracks per 10^6 POT in MC.

- $p > 10$ GeV/c is required to make sure no other particle is left rather than pion or muon. This will also reduce the effect of multiple scattering.
- The track must be in RPC acceptance and has no associated hits beyond the first RPC layer.
- $z_{vertex} < 51$ cm is required to reduce the effect of fake vertices.
- $p_T > 0.3$ GeV/c is required to improve the peak in the invariant mass.
- $\chi^2/nDof < 5$.
- doca < 5 cm.

Arming with these, the invariant mass of two pion events in the data can be retrieved.

5.2.2 Invariant Mass

The invariant mass of two pion events has been plotted for both intermediate and nomial field data and presented in Figure 5.16. A fit with a crystal ball function was superimposed. The Crystall Ball function is defined as [28]

$$f(x;\alpha,n,\bar{x},\sigma) = N \cdot \begin{cases} exp(-\frac{(x-\bar{x})^2}{2\sigma^2}) & \frac{x-\bar{x}}{\sigma} \geq -\alpha \\ A \cdot (B - \frac{(x-\bar{x})}{\sigma})^{-n} & \frac{x-\bar{x}}{\sigma} \leq \alpha \end{cases} \tag{5.4}$$

where A and B are defined as, $A = (\frac{n}{|\alpha|})^n \cdot \exp(-\frac{|\alpha|^2}{2})$ and $B = \frac{n}{|\alpha|} - |\alpha|$

In the nominal field data, no peak accounting for the K^0_S is observed. The peak around $\sim$ 8.4 GeV$/c^2$ might be due to the same peak in the MC as well as combinatorial background of muons and pions. In the intermediate field data, the number of observed events is very low. This result, in fact, is not surprising as it is not excluded by our MC. Furthermore, the expected number of V0 events was very low indeed.

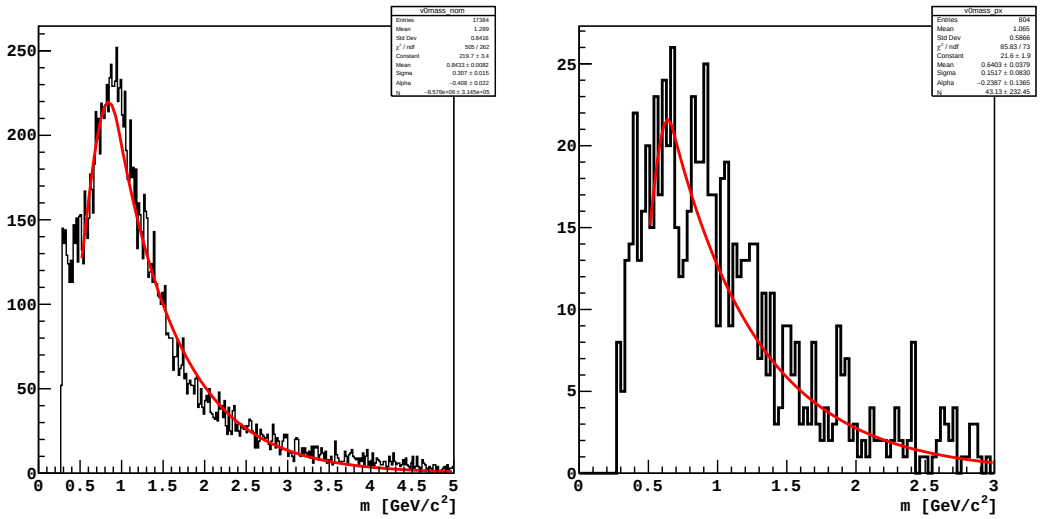

Figure 5.16: Invariant mass-data.

CHAPTER 6

CONCLUSION

This thesis is devoted to searching for K_S^0 decays in the muon flux test beam data.

The most significant background for the SHiP experiment is the so-called V0 decays i.e. decays of Λ, K_L^0, and K_S^0. Their signatures in the SHiP detector resemble to SHiP's new physics channels. These particles can be produced by muon interaction with the material surrounding the SHiP detector. Among V0 decays, neutral kaons rank top among other background sources. The SHiP test beam has provided an opportunity to study the K_S^0 production with muon deep inelastic scattering. Motivating from this, we put efforts into search for such events in the SHiP test beam data.

The production of K_S^0 is simulated with deep inelastic scattering of muons inside the iron. These events were further processed with GEANT4. The signal for the K_S^0 is two oppositely charged pions identified in detectors.

While seeing a clear peak around the nominal mass of the K_S^0 in the standalone production it is understood that low momenta of pions originated from muon induced K_S^0 leads to a low number of reconstructed decay vertices. Another production involving other deep inelastic scattering products were done. In this simulation K_S^0 peak was not isolated from other sources. New selection criteria are applied to improve the K_S^0 identification. However, the background still dominates over the signal.

In order to tag pion tracks, RPC response of pions were simulated with GEANT4. The signature obtained from pions in this simulation is used in the data to distinguish pions from muons. As far as the data is concerned, the analysis gets more complicated. Shortcomings of the data for the K_S^0 search are the background and the lack of luminosity. The luminosity does not provide enough statistics to observe a significant

number of muon DIS events. The background, on the other hand, is much larger in the data. It's mainly due to the fake reconstruction of vertices. This is explained as the very low opening angle of two tracks leads tracks to share the same hit in the first tracking station. Another remark should be made for particle identification. In the data, anything not muon is counted as a pion. However, this identification might not seperate good enough muons from pions. Furthermore, there might be tracks associated with electrons, positrons, protons and charged kaons.

It's going to be incorrect if one deduces a direct result from this work. The indirect result, on the other hand, no K_S^0 decay is observed in the muon flux test beam data as expected.

To have a better knowledge of muon induced V0 events it might be needed to perform another test beam with several modifications to muon flux setup. The p_T acceptance of detectors can be increased by modifying the geometry of the spectrometer. Particle identification should be extended with calorimetry as well. Luminosity should also be increased.

At the end of the day, this is good news for the SHiP experiment as the the term "signal" in the context of this work is actually the "background" for SHiP.

REFERENCES

[1] M. Anelli *et al.*, "A Facility to Search for Hidden Particles (SHiP) at the CERN SPS," Tech. Rep. CERN-SPSC-2015-016. SPSC-P-350. arXiv:1504.04956, CERN, Geneva, Apr 2015. Technical Proposal.

[2] C. Ahdida *et al.*, "SHiP Experiment - Comprehensive Design Study report," Tech. Rep. CERN-SPSC-2019-049. SPSC-SR-263, CERN, Geneva, Dec 2019.

[3] C. Grupen and B. Schwartz, *Particle detectors*, vol. 26. Cambridge, UK: Cambridge Univ. Pr., 2008.

[4] M. S. AL-Buriahi, M. T. Ghoneim, and M. T. Hussein, "Production of charged hadrons in muon deep inelastic scattering," *Chinese Journal of Physics*, vol. 54, no. 5, pp. 802 – 809, 2016.

[5] R. Aaij *et al.*, "Observation of structure in the J/ψ-pair mass spectrum," 6 2020.

[6] Y. Fukuda *et al.*, "Evidence for oscillation of atmospheric neutrinos," *Phys. Rev. Lett.*, vol. 81, pp. 1562–1567, 1998.

[7] A. Sakharov, "Baryon asymmetry of the universe," *Sov. Phys. Usp.*, vol. 34, no. 5, pp. 417–421, 1991.

[8] J. Silk *et al.*, *Particle Dark Matter: Observations, Models and Searches*. Cambridge: Cambridge Univ. Press, 2010.

[9] S. Alekhin *et al.*, "A facility to Search for Hidden Particles at the CERN SPS: the SHiP physics case," Tech. Rep. CERN-SPSC-2015-017. SPSC-P-350-ADD-1, CERN, Geneva, Apr 2015. 200 pages + appendices/references.

[10] C. Ahdida *et al.*, "Sensitivity of the SHiP experiment to Dark Photons," *Manuscript in preparation*, 2020.

[11] C. Ahdida *et al.*, "Measurement of the muon flux from 400 GeV/c protons interacting in a thick molybdenum/tungsten target," Tech. Rep. arXiv:2001.04784, CERN, Geneva, Mar 2020.

[12] R. Acquafredda *et al.*, "The OPERA experiment in the CERN to Gran Sasso neutrino beam," *JINST*, vol. 4, p. P04018, 2009.

[13] C. Ahdida *et al.*, "SND@LHC," 2 2020.

[14] M. Al-Turany, D. Bertini, R. Karabowicz, D. Kresan, P. Malzacher, T. Stockmanns, and F. Uhlig, "The FairRoot framework," *Journal of Physics: Conference Series*, vol. 396, p. 022001, dec 2012.

[15] R. Brun and F. Rademakers, "Root — an object oriented data analysis framework," *Nuclear Instruments and Methods in Physics Research Section A: Accelerators, Spectrometers, Detectors and Associated Equipment*, vol. 389, no. 1, pp. 81 – 86, 1997. New Computing Techniques in Physics Research V.

[16] S. Agostinelli *et al.*, "Geant4—a simulation toolkit," *Nuclear Instruments and Methods in Physics Research Section A: Accelerators, Spectrometers, Detectors and Associated Equipment*, vol. 506, no. 3, pp. 250 – 303, 2003.

[17] T. Sjostrand, S. Mrenna, and P. Z. Skands, "PYTHIA 6.4 Physics and Manual," *JHEP*, vol. 05, p. 026, 2006.

[18] T. Sjöstrand, S. Ask, J. R. Christiansen, R. Corke, N. Desai, P. Ilten, S. Mrenna, S. Prestel, C. O. Rasmussen, and P. Z. Skands, "An introduction to pythia 8.2," *Computer Physics Communications*, vol. 191, pp. 159 – 177, 2015.

[19] C. Andreopoulos, "The GENIE neutrino Monte Carlo generator," *Acta Phys. Polon. B*, vol. 40, pp. 2461–2475, 2009.

[20] D. Bick *et al.*, "Alignment of the muon-flux spectrometer in FairShip using the survey measurements," tech. rep., CERN, Feb 2019.

[21] D. Bick, *Setup of a drift tube muon tracker and calibration of muon tracking in Borexino*. PhD thesis, Hamburg U., 2011.

[22] C. C. Ahdida *et al.*, "Measurement of the muon flux for the SHiP experiment," tech. rep., CERN, Dec 2019.

[23] J. Rauch and T. Schlüter, "GENFIT — a generic track-fitting toolkit," *Journal of Physics: Conference Series*, vol. 608, p. 012042, may 2015.

[24] J. Batley *et al.*, "A Measurement of the CP-conserving component of the decay K0(S) —> pi+ pi- pi0," *Phys. Lett. B*, vol. 630, pp. 31–39, 2005.

[25] J. Batley *et al.*, "Precision measurement of the ratio $BR(K_S \to \pi^+\pi^-e^+e^-)/BR(K_L\pi^+pi^-\pi^0_D)$," *Phys. Lett. B*, vol. 694, pp. 301–309, 2011.

[26] K. Olive *et al.*, "Review of Particle Physics," *Chin. Phys. C*, vol. 38, p. 090001, 2014.

[27] C. Lippmann, "Particle identification," *Nucl. Instrum. Methods Phys. Res., A*, vol. 666, pp. 148–172. 61 p, Jan 2011. 61 pages, 30 figures.

[28] T. Skwarnicki, *A study of the radiative CASCADE transitions between the Upsilon-Prime and Upsilon resonances*. PhD thesis, Cracow, INP, 1986.